โคพอลิเมอร์ไรเซชันของเอทิลีนกับหนึ่งโอเลฟินบนตัวเร่งปฏิกิริยาเมทัลโลซีนที่รองรับด้วยไทเทเนีย

นายธนัย ศรีไพศาล

วิทยานิพนธ์นี้เป็นส่วนหนึ่งของการศึกษาตามหลักสูตรปริญญาวิศวกรรมศาสตรมหาบัณฑิต
สาขาวิชาวิศวกรรมเคมี ภาควิชาวิศวกรรมเคมี
คณะวิศวกรรมศาสตร์ จุฬาลงกรณ์มหาวิทยาลัย
ปีการศึกษา 2551

COPOLYMERIZATION OF ETHYLENE/1-OLEFIN OVER TITANIA-SUPPORTED METALLOCENE CATALYST

Mr. Thanai Sriphaisal

A Thesis Submitted in Partial Fulfillment of the Requirements
for the Degree of Master of Engineering Program in Chemical Engineering
Department of Chemical Engineering
Faculty of Engineering
Chulalongkorn University
Academic Year 2008

Thesis Title	COPOLYMERIZATION OF ETHYLENE/1-OLEFIN OVER TITANIA-SUPPORTED METALLOCENE CATALYST
By	Mr. Thanai Sriphaisal
Field of Study	Chemical Engineering
Advisor	Assistant Professor Bunjerd Jongsomjit, Ph.D.

Accepted by the Faculty of Engineering, Chulalongkorn University in Partial Fulfillment of the Requirements for the Master's Degree

..... Dean of the Faculty of Engineering
(Associate Professor Boonsom Lerdhirungwong, Dr.Ing.)

THESIS COMMITTEE

..... Chairman
(Assistant Professor Montree Wongsri, D.Sc.)

..... Advisor
(Assistant Professor Bunjerd Jongsomjit, Ph.D.)

..... Examiner
(Associate Professor ML. Supakanok Thongyai, Ph.D.)

..... External Examiner
(Assistant Professor Sirirat Wacharawichanant, D.Eng.)

ธนัย ศรีไพศาล : โคพอลิเมอร์ไรเซชันของเอทิลีนกับหนึ่งโอเลฟินบนตัวเร่งปฏิกิริยาเมทัลโลซีนที่รองรับด้วยไทเทเนีย (COPOLYMERIZATION OF ETHYLENE/1-OLEFIN OVER TITANIA-SUPPORTED METALLOCENE CATALYST) อ. ที่ปรึกษาวิทยานิพนธ์หลัก : ผศ. ดร. บรรเจิด จงสมจิตร, 83 หน้า.

เนื่องจากตัวเร่งปฏิกิริยาเมทัลโลซีนกำลังได้รับความสนใจในธุรกิจเชิงพาณิชย์สำหรับในการพอลิเมอร์ไรเซชันของโอเลฟิน จึงทำให้ตัวเร่งปฏิกิริยาเมทัลโลซีนถูกนำไปศึกษาอย่างแพร่หลายเพื่อทำให้ตัวเร่งปฏิกิริยานี้มีประสิทธิภาพมากที่สุด ซึ่งเป็นที่รู้กันว่าพอลิเอทิลีนความหนาแน่นต่ำแบบโซ่ตรงสามารถสังเคราะห์ได้จากการโคพอลิเมอร์เซชันของเอทิลีนกับหนึ่งโอเลฟินโดยใช้ตัวเร่งปฏิกิริยาเมทัลโลซีน แต่ถึงอย่างไรก็ตามการสังเคราะห์พอลิเมอร์ชนิดดังกล่าวโดยตัวเร่งปฏิกิริยาเมทัลโลซีนในระบบที่ไม่มีตัวรองรับยังคงมีข้อเสียอยู่ 2 ข้อ คือไม่สามารถควบคุมโครงสร้างสัณฐานของพอลิเมอร์ที่ผลิตได้และเกิดสิ่งสกปรกติดที่เครื่องปฏิกรณ์ ดังนั้นตัวเร่งปฏิกิริยาในระบบที่มีตัวรองรับจึงถูกนำมาใช้เพื่อแก้ไขปัญหาดังกล่าว ในงานวิจัยนี้แสดงให้เห็นถึงผลกระทบของไทเทเนียที่ถูกใช้เป็นตัวรองรับสำหรับตัวเร่งปฏิกิริยาเซอร์โคโนซีนโดยวิธีอินซิตูโคพอลิเมอร์ไรเซชันของเอทิลีนกับหนึ่งเฮกซีนเพื่อผลิตพอลิเอทิลีนความหนาแน่นต่ำแบบโซ่ตรง ในขั้นแรกโมดิฟายเมทิลอะลูมินอกเซนแห้ง (dMMAO) จะถูกเคลือบฝังบนตัวรองรับไทเทเนียเฟสต่างๆหลังจากนั้นนำไปวิเคราะห์ด้วยเครื่อง XPS, SEM/EDX และ ICP/AES พบว่าปริมาณอะลูมินาในโมดิฟายเมทิลอะลูมินอกเซนแห้งจะอยู่กันมากบริเวณด้านนอกหรือภายนอกพื้นผิวของตัวรองรับไทเทเนีย มีการกระจายตัวที่ดีของโมดิฟายเมทิลอะลูมินอกเซนแห้งบนตัวรองรับไทเทเนียเมื่อดูด้วย SEM/EDX โคพอลิเมอร์ที่ได้จะถูกนำไปวิเคราะห์ด้วย DSC, SEM/EDX และ ^{13}C NMR ความว่องไวในการเกิดปฏิกิริยาจะสูงสุดเมื่อใช้ไทเทเนียเฟสอนาเทสเนื่องจากอันตรกิริยาที่เหมาะสมระหว่างตัวรองรับและตัวเร่งปฏิกิริยาร่วมดังที่เห็นได้จาก TGA โคพอลิเมอร์ที่ได้เป็นโคพอลิเมอร์แบบสุ่มที่มีไทรแอดดิสทริบิวชันที่ต่างกันดังที่พิสูจน์ได้จาก ^{13}C NMR

ภาควิชา.....วิศวกรรมเคมี..... ลายมือชื่อนิสิต.....ธนัย ศรีไพศาล.....

สาขาวิชา.....วิศวกรรมเคมี..... ลายมือชื่ออ. ที่ปรึกษาวิทยานิพนธ์หลัก .....

ปีการศึกษา.....2551.....

##5070563921: MAJOR CHEMICAL ENGINEERING
KEYWORDS: SUPPORTED METALLOCENE CATALYST/BIMODAL/ TITANIA/ COPOLYMERIZATION OF ETHYLENE/ ZIRCONOCENE/ 1-HEXENE

THANAI SRIPHAISAL: COPOLYMERIZATION OF ETHYLENE/1-OLEFIN OVER TITANIA-SUPPORTED METALLOCENE CATALYST ADVISOR: ASST. PROF. BUNJERD JONGSOMJIT, Ph.D., 82 pp.

Because of the commercial interest of using metallocene catalysts for olefin polymerization, it has led to an extensive effort for utilizing metallocene catalysts more efficiently. It is known that linear low-density polyethylene (LLDPE) can be synthesized by copolymerization of ethylene and 1-olefins using metallocene catalysts. However, it was found that homogenization of metallocene has two major disadvantages; the lack of morphology control of polymers produced and reactor fouling. Therefore, heterogenization of metallocene was brought to solve these problems. This present study reveals the effect of TiO_2 as a support for zirconocene/dMMAO catalyst on *in situ* copolymerization of ethylene/1-hexene in order to produce the linear low-density polyethylene (LLDPE). First, the dMMAO was impregnated onto various phases of TiO_2 supports, and then characterized by XPS, SEM/EDX and ICP/AES. It was found that the $[Al]_{dMMAO}$ is located mostly on the outer or external surface of TiO_2 supports. The $[Al]_{dMMAO}$ distribution on the TiO_2 supports is good as seen by SEM/EDX. The copolymer obtained was further characterized by DSC, SEM/EDX and ^{13}C NMR. The highest activity occurred when the anatase phase of TiO_2 was employed due to the optimal interaction between the support and cocatalyst as seen by TGA. The copolymer obtained were random copolymer having different triad distribution as proven by ^{13}C NMR.

Department :...Chemical Engineering... Student's Signature.....
Field of Study : ..Chemical Engineering. Advisor's Signature.....
Academic Year : ..2008.....

ACKNOWLEDGEMENTS

The author would like to express my greatest gratitude and appreciation to Assistant Professor Dr. Bunjerd Jongsomjit, my advisor, for his invaluable suggestions, encouragement during my study and useful discussions throughout this research. His advice is always worthwhile and without him this work could not be possible.

I wish to thank Assistant Professor Dr. Montree Wongsri, as the chairman, Associate Professor Dr. ML. Supakanok Thongyai and Assistant Professor Dr. Sirirat Wacharawichanant as the members of the thesis committee for their valuable guidance and revision throughout my thesis.

Sincere thanks are given to the graduate school and department of chemical engineering at Chulalongkorn University for the financial support of this work. And many thanks are given to PTT Chemical Public Company Limited for ethylene gas supply and MEKTEC Manufacturing Corporation (Thailand) Limited for DSC and NMR measurements.

Many thanks for kind suggestions and useful help to Mr. Wathanyoo Owpradit, Mr. Pongsathorn Wongwaiwattanakul, Mr. Ekrachan Chaichana and many friends in the Center of Excellence on Catalysis and Catalytic Reaction Engineering, Department of Chemical Engineering, Faculty of Engineering, Chulalongkorn University for friendship and their assistance especially the members of Z&M group. To the many others, not specifically named, who have provided me with support and encouragement, please be assured that I thinks of you.

Finally, I would like to express my highest gratitude to my family and who are always beside me and support throughout this study.

CONTENTS

Page

Page

Page

LIST OF TABLES

Table Page

LIST OF FIGURES

Figure Page

Figure Page

CHAPTER I

INTRODUCTION

It is known that polymer is very important for engineering plastic and medical device because it has a very useful property, such as light weight, prevent liquid leak, hard to decay, low fabrication cost and easy to process. Polyethylene is one of the most widely used in many applications such as films, house wares, bottles, containers, pipe, tubing, wire and cable insulation, conduits and coating [1]. Actually, the density of polyethylene is a key used to classify the application of polyethylene [2] and it can be controlled by altering the degree of branching in the polymer chain. The catalytic polymerization of ethylene with alfa olefins is a typical way to introduce the short-chain branching into the polymer backbone to produce linear low-density polyethylene (LLDPE) [2]. LLDPE is widely used in many applications, especially, for plastic films [3]. The driving force in the LLDPE growth can be attributed to metallocene-catalyzed LLDPE resin. The demand for metallocene-catalyzed polyethylene is predicted to increase 45% between 1996 and 2000 and eventually grow to 5.9 million tons in the year 2010 [4].

In 1957, Natta and Breslow discovered the first homogeneous Ziegler-Natta catalyst [5]. The ethylene polymerization with titanocene catalyst Cp_2TiCl_2 and the alkylaluminum chloride as cocatalyst exhibited a low polymerization activity. In 1980's, new cocatalyst was discovered by Kaminsky and coworkers [6]. While studying a homogeneous $Cp_2ZrCl_2/Al(CH_3)_3$ polymerization system, water was unexpected introduced into the reactor leading to an utmost active ethylene polymerization system. The hydrolysis of the trimethylaluminum, $Al(CH_3)_3$ is cause of formation the cocatalyst methylaluminoxane (MAO) which precede to the high activity [5].

Metallocene catalyst systems gave high activity, excellent stereoregularity in 1-olefins polymerization [1,7,8] and frequently produced the polymer with narrow molar mass distribution of approximately two [9-11]. However, the main disadvantage of these catalyst systems is lack of morphology control and reactor

fouling [7]. The way to overcome these drawbacks is to bind the metallocene catalyst onto inorganic supports [12,13]. These heterogeneous catalytic system can be eliminate the minor disadvantage, such as the requirement of high aluminum-to-transition metal molar ratios and extensive polymer washing [14]. The other advantage of supported metallocene catalyst system is that it can be adjusted to suitable for industrial applications such as gas- and slurry-phase polymerization processes [14]. In general, many metallocene catalysts are supported on inorganic carriers, such as carbon nanotube, SiO_2, Al_2O_3, $MgCl_2$ and TiO_2 [15-28]. Titania was studied a little for modified silica and a few papers was used titania as support compared with another based acidic oxide.

The main objective of this work was to investigate the influence of phase composition in TiO_2 supports on the catalytic activity and polymer properties. The TiO_2 supports having different phases, such as, anatase, rutile and mixed phases were employed as supports for zirconocene/dMMAO catalysts. The properties of the supports were characterized using N_2 physisorption, X-ray diffraction (XRD), scanning electron microscope/energy dispersive X-ray spectroscopy (SEM/EDX), inductively coupled plasma atomic emission spectrometer (ICP-AES) and thermal gravimetric analysis (TGA). The obtained copolymer was characterized by ^{13}C-nuclear magnetic resonance (^{13}C-NMR), SEM/EDX and differential scanning calorimeter (DSC).

This thesis was divided into five chapters. Chapter I involved an overview of the use of metallocene catalyst for the polyolefin industry. In Chapter II, knowledge and open literature dealing with metallocene catalysis for olefin polymerization were presented. The literature review was accentuated metallocene catalyst system used for copolymerization of ethylene with α-olefins. The experimental procedure as well as the instrument and techniques used for characterizing the resulting polymers were also described in Chapter III.

In Chapter IV, the results on ethylene and α-olefins copolymerization using various TiO_2 supported zirconocene/dMMAO catalysts were presented. The influences of various phases of support on the catalytic activity and polymer

properties were investigated. The characteristics support and catalyst precursors using N_2 physisorption, X-ray diffraction (XRD), Thermogravimetric analysis (TGA), Scanning electron microscopy (SEM), Energy-dispersive x-ray spectrometer (EDX), X-ray photoelectron spectroscopy (XPS) and inductively coupled plasma atomic emission spectrometer (ICP-AES) and obtained copolymer using Differential scanning calorimetry (DSC), Scanning electron microscopy (SEM), Energy-dispersive x-ray spectrometer (EDX) and ^{13}C-nuclear magnetic resonance (^{13}C – NMR).

Finally, conclusions of this work and some recommendations for future research work were provided in Chapter V.

CHAPTER II

LITERATURE REVIEW

2.1 Polymerization of olefins

Until 1953, processes for olefin polymerization were based on a radical process at high pressures and high temperatures. Polymerization of ethylene under these conditions (2000-3000 bars; 150-230 °C) yields low-density polyethylene (LDPE, **Figure 2.1**), a low melting and highly branched polyethylene, containing both long- and short chain branches [29]. With propylene only atactic , low molecular weight material can be obtained. Ziegler found that ethylene could also be polymerized using $TiCl_4$ and alkylsaluminium. The process yields linear polyethylene (HDPE, **Figure 2.1**) with a high molecular weight. Natta proved that the same type of catalyst also polymerizes propylene [30]. The resulting polymer mixture is predominantly isotactic with additional polymer fractions that are of a lower stereoregularity or atactic. Copolymerizations of ethylene with 1-hexene/1-octene with the titanium Ziegler catalysts result in copolymers in which the degree of incorporation of the α-olefin varies over the molecular weight distribution. Upon reaction of a vanadium compound, e.g. $V(acac)_3$ (acac = acetylacetonato) or VCl_4, with an alkylaluminium cocatalyst a catalyst for the production of EP (copolymer of ethylene and propylene) and EPDM (ethylene-propylene-diene elastomers) is obtained [31]. The homogeneous system shows high initial activity, but is rapidly deactivated [32]. An important advantage is that the comonomers are randomly incorporated in the polymer over the full range of the molecular weight distribution.

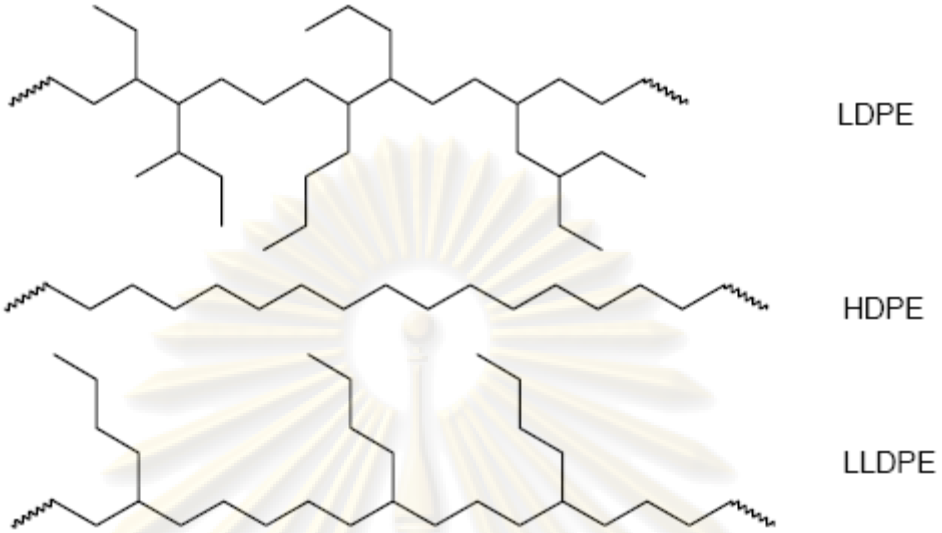

Figure 2.1 Examples of polyethenes: LDPE, HDPE and LLDPE (copolymer of ethene and 1-hexene)

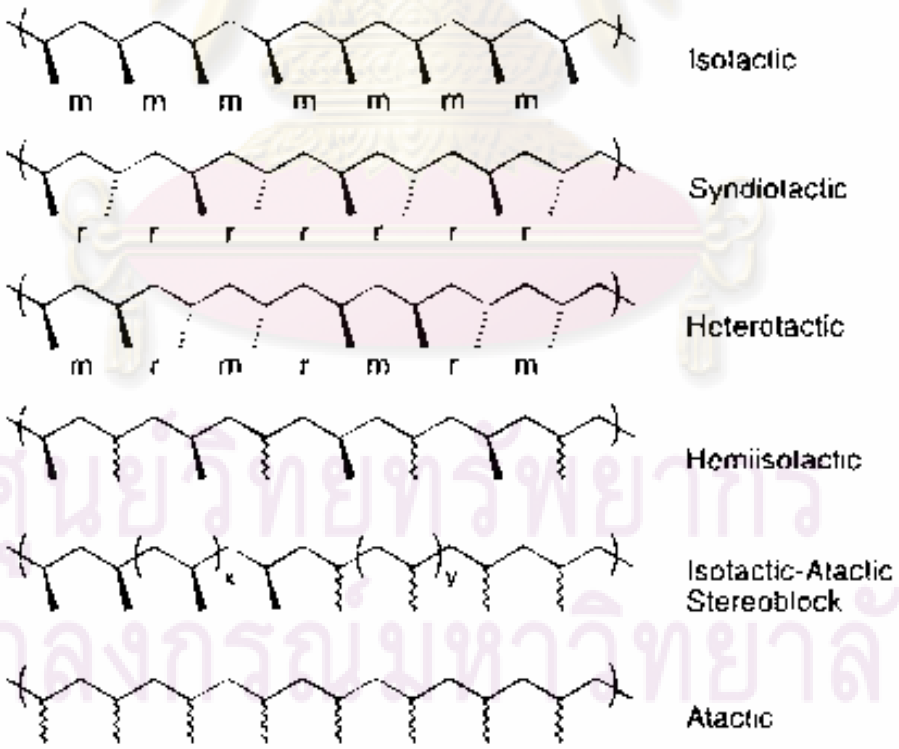

Figure 2.2 Common polymer tacticities [33]

The heterogeneity of Z-N (Ziegler Natta) systems and Phillips/Union Carbide type catalysts makes them very attractive for industrial application, and most polyolefin materials are still produced by means of heterogeneous catalysts [34]. These heterogeneous systems combine high activity with an easy process ability of the resulting product mixture and good polymer particle morphology. The catalyst systems contain various types of active sites with different geometries and activities, which often leads to polymers with broad or polymodal molecular weight distributions or to mixtures of different types of polymers (e.g. mixtures of atactic and isotactic polypropene) [35]. Many improvements on the classical Z-N type catalysts have been made over the last 30 years, and modern Z-N systems allow a much better control of polymer properties. Most of these improvements were achieved by empirical methods [36].

In 1957 the first articles on homogeneous titanium-based olefin polymerization were published by Breslow and Newburg [5] and by Natta, Pino and co-workers [37]. When reacting Cp_2TiCl_2 with Et_2AlCl (DEAC) under conditions similar to those used with Z-N systems, a catalyst that polymerizes ethylene is obtained. The first homogeneous systems showed a low activity, when compared to classical Z-N systems and were also not active in polymerization of higher olefins. In contrast to heterogeneous systems, homogeneous catalysts have a single type of well-defined active sites. Although heterogeneous catalysts are in general industrially more practical, a higher control of properties of the catalyst, and more detailed kinetic and mechanistic studies are possible with well-defined molecular catalysts (“single site” catalysts) [6].

2.2 Mechanisms of homogeneous, catalytic olefin polymerization

The geometric and electronic structure of the active species affect the properties of the resulting polymer, such as molecular weight, molecular weight distribution, region and stereoselectivity (for the homopolymerization of α-olefins) and the incorporation of the other monomers. (for copolymerizations).

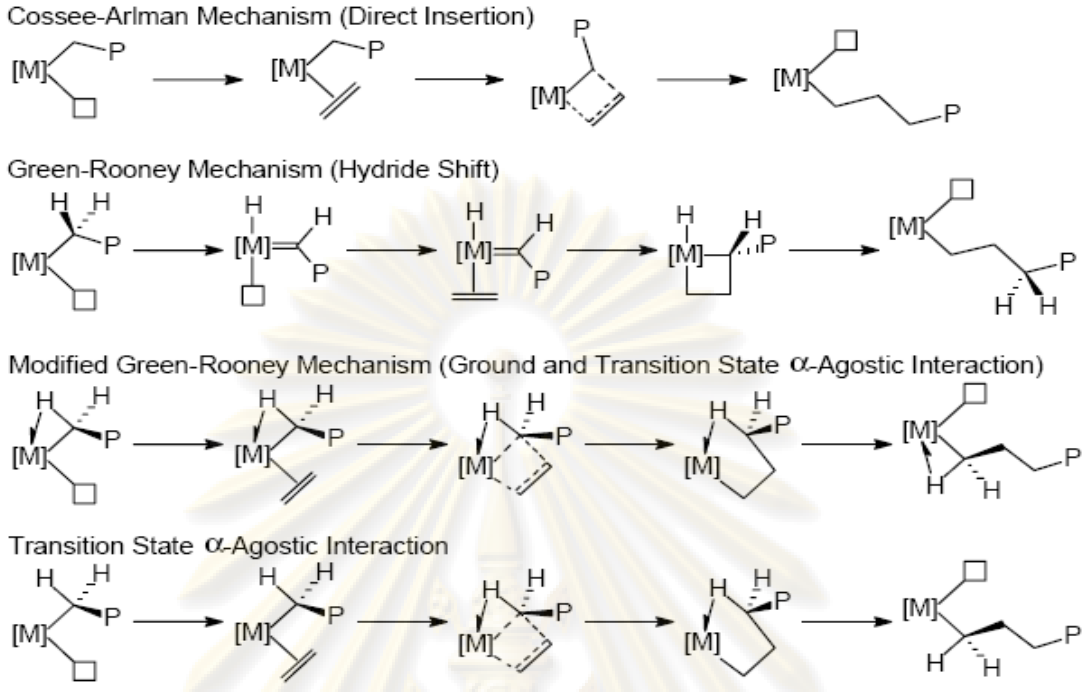

Figure 2.3 Scheme of migratory insertion mechanism, in which the metal-bound alkyl group migrates to the alkene

It is now generally accepted that this active species is an electron deficient, preferably cationic metal alkyl species. For heterogeneous systems the active sites are at dislocations and edges of the crystals, for homogeneous catalysts the active site is enclosed by a set of ancillary ligands. The cationic metal species are electronically balanced by a preferably weakly nucleophilic, weakly coordinating counter anion. Cossee and Arlman were the first to propose a mechanism for catalytic olefin polymerization [38]. They proposed that the polymer chain is growing via a *cis*-insertion of the olefin into a metal-carbon bond, migratory insertion mechanism, in which the metal-bound alkyl group migrates to the alkene shown in **Figure 2.3**

2.2.1 Chain transfer - molecular weight and molecular weight distribution

Besides chain growth, chain transfer processes are also important in olefin polymerization. The rate of chain growth over chain transfer determines molecular weight and molecular weight distribution of the resulting polymer, which are important factors for material and processing properties. These rates are

determined by the catalytic centre and its surrounding ligand (and sometimes by the cocatalyst), and they provide essential information about the polymerization mechanism.

For chain transfer several mechanisms have been revealed, which include termination reactions by β-H, β-CH_3 and H-transfer to monomer (**Figure 2.4**) chain transfer to aluminum (e.g. when an aluminum activator or scavenger is used, (**Figure 2.5**), and σ-bond metathesis between the M-alkyl bond and a C-H bond of an alkene or a solvent molecule. Also chain transfer between catalyst active sites has been suggested (in a dual site ethene/1-hexene copolymerisation).

In industrial polyolefin production, often chain transfer agents such as H_2 are added to the polymerizing mixture to gain a better control of polymer molecular weights [39]. In absence of alkylaluminium the main mechanism for chain transfer is via β-H abstraction. Two different mechanisms for β-H abstraction have been observed (**Figure 2.4**), which differ in the rate determining step (r.d.s.) of the chain transfer. In both cases polymers are obtained with olefinic end-groups. When the β-H transfer to monomer is rate determining (route 1, **Figure 2.4**), the rate of chain termination increases with increasing olefin concentration. Since also the chain growth (rate of insertion) is 1st order in olefin, molecular weights are independent of monomer concentration for these systems. When the rate determining step is the β-H transfer to metal (route 2, **Figure 2.4**) the rate of termination is independent of monomer concentration (0th order in olefin), and molecular weights increase with increasing monomer concentration. When MAO or other alkyls aluminium is present in the reaction medium, another mechanism of chain transfer can be observed. Especially in MAO with a high Me_3Al (TMA) content a considerable amount of chain transfer to aluminum may occur although this transmetallation has also been observed in TMA-free MAO [40]. As opposed to the mechanisms responsible for chain transfers to monomer, which give olefinic end groups, chain transfers to aluminum give, after hydrolysis, polymers with aliphatic end groups.

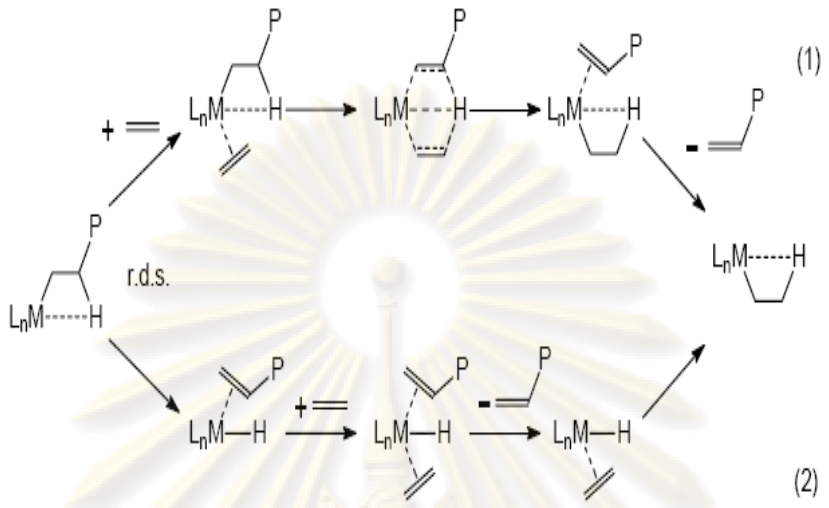

Figure 2.4 Scheme of termination reactions by β-H, β-CH_3 and H-transfer to monomer

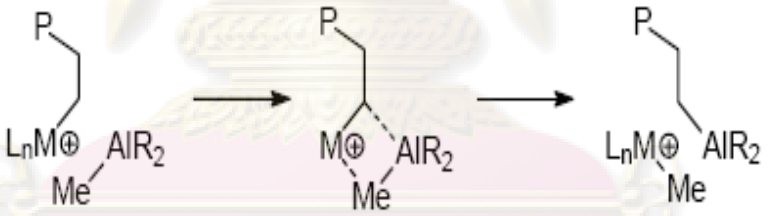

Figure 2.5 Scheme of chain transfer to aluminum

2.3 Background on Polyolefin Catalysts

Polyolefins can be produced with free radical initiators, Phillips type catalysts, Ziegler-Natta catalysts and metallocene catalysts. Ziegler-Natta catalysts have been most widely used because of their broad range of application. However, Ziegler-Natta catalyst provides polymers having broad molecular weight distribution (MWD) and composition distribution due to multiple active sites formed [41].

Metallocene catalysts have been used to polymerize ethylene and -olefins commercially. The structural change of metallocene catalysts can control composition distribution, incorporation of various comonomers, MWD and stereoregularity [42].

2.3.1 Catalyst Structure

Metallocene is a class of compounds in which cyclopentadienyl or substituted cyclopentadienyl ligands are π-bonded to the metal atom. The stereochemistry of biscyclopentadienyl (or substituted cyclopentadienyl)-metal bis (unibidentate ligand) complexes can be most simply described as distorted tetrahedral, with each η^5-L group (L = ligand) occupying a single co-ordination position, as in **Figure 2.6** [43].

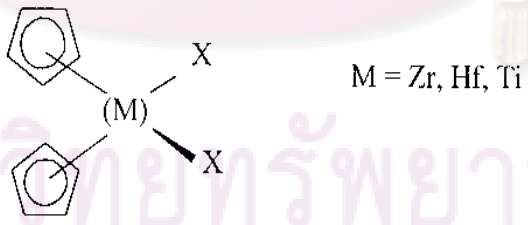

Figure 2.6 Molecular structure of metallocene

Representative examples of each category of metallocenes and some of zirconocene catalysts are shown in **Table 2.1** and **Figure 2.7**, respectively.

Table 2.1 Representative Examples of Metallocenes **[43]**

Category of metallocenes	Metallocene Catalysts
[A] Nonstereorigid metallocenes	1) Cp_2MCl_2 (M = Ti, Zr, Hf) 2) Cp_2ZrR_2 (M = Me, Ph, CH_2Ph, CH_2SiMe_3) 3) $(Ind)_2ZrMe_2$
[B] Nonstereorigid ring-substituted metallocenes	1) $(Me_5C_5)_2MCl_2$ (M = Ti, Zr, Hf) 2) $(Me_3SiCp)_2ZrCl_2$
[C] Stereorigid metallocenes	1) $Et(Ind)_2ZrCl_2$ 2) $Et(Ind)_2ZrMe_2$ 3) $Et(IndH_4)_2ZrCl_2$
[D] Cationic metallocenes	1) $Cp_2MR(L)^+[BPh_4]^-$ (M = Ti, Zr) 2) $[Et(Ind)_2ZrMe]^+[B(C_6F_5)_4]^-$ 3) $[Cp_2ZrMe]^+[(C_2B_9H_{11})_2M]^-$ (M = Co)
[E] Supported metallocenes	1) Al_2O_3-$Et(IndH_4)_2ZrCl_2$ 2) $MgCl_2$-Cp_2ZrCl_2 3) SiO_2-$Et(Ind)_2ZrCl_2$

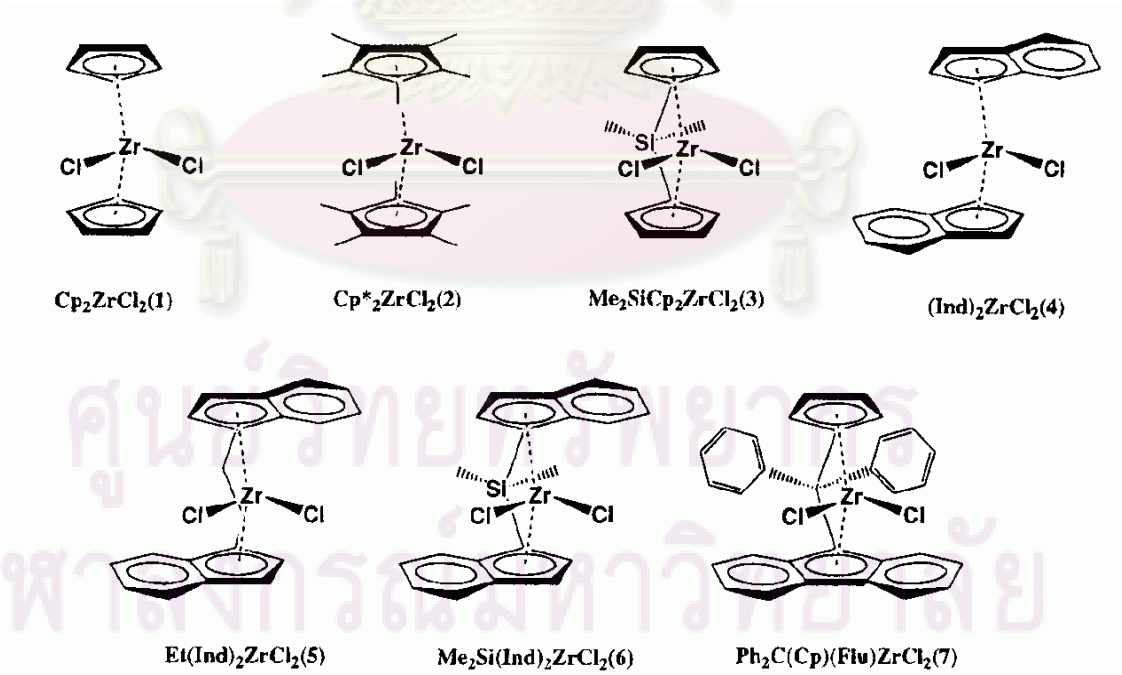

Figure 2.7 Some of zirconocene catalysts structure [44]

Composition and types of metallocene have several varieties. When the two cyclopentadienyl (Cp) rings on either side of the transition metal are unbridged, the metallocene is nonstereorigid and it is characterized by C_{2v} symmetry. The Cp_2M (M = metal) fragment is bent back with the centroid-metal-centroid angle θ about 140° due to an interaction with the other two σ bonding ligands [45]. When the Cp rings are bridged (two Cp rings arranged in a chiral array and connected together with chemical bonds by a bridging group), the stereorigid metallocene, so-called ansa-metallocene, could be characterized by either a C_1, C_2, or C_s symmetry depending upon the substituents on two Cp rings and the structure of the bridging unit as schematically illustrated in **Figure 2.8** [43].

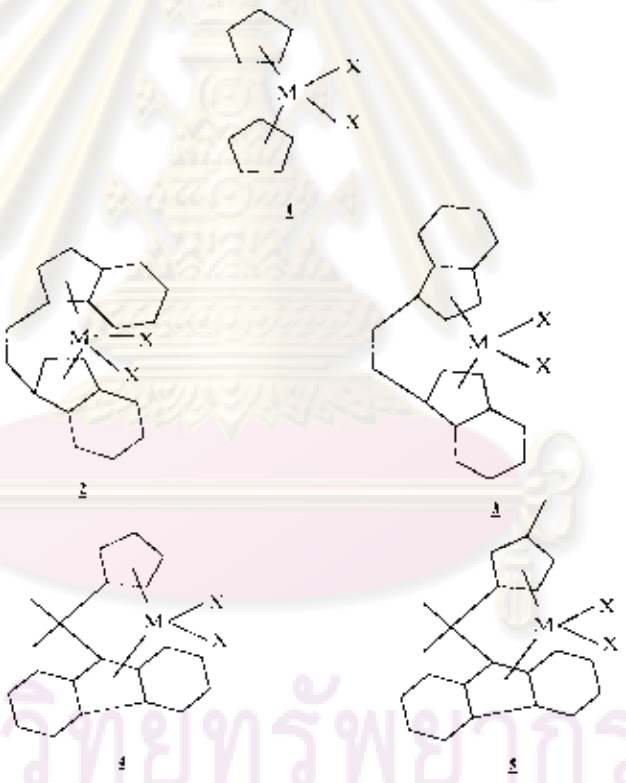

Figure 2.8 Scheme of the different metallocene complex structures [43]. Type 1 is C_{2v}-symmetric; Type 2 is C_2-symmetric; Type 3 is C_s-symmetric; Type 4 is C_s-symmetric; Type 5 is C_1-symmetric.

2.3.2 Polymerization Mechanism

The mechanism of catalyst activation is not clearly understood. However, alkylation and reduction of the metal site by a cocatalyst (generally alkyl aluminum or alkyl aluminoxane) is believed to generate the cationic active catalyst species.

First, in the polymerization, the initial mechanism started with formation of cationic species catalyst that is shown below.

Initiation

$$Et(Ind)_2ZrCl_2 + Al(CH_3)_3 \longrightarrow Et(Ind)_2ZrClMe + Al(CH_3)_2Cl$$

Propagation proceeds by coordination and insertion of new monomer unit in the metal carbon bond. Cossee mechanism is still one of the most generally accepted polymerization mechanism (**Figure 2.9**) [46]. In the first step, monomer forms a complex with the vacant coordination site at the active catalyst center. Then through a four-centered transition state, bond between monomer and metal center and between monomer and polymer chain are formed, increasing the length of the polymer chain by one monomer unit and generating another vacant site.

Figure 2.9 Cossee mechanism for Ziegler-Natta olefin polymerization [46].

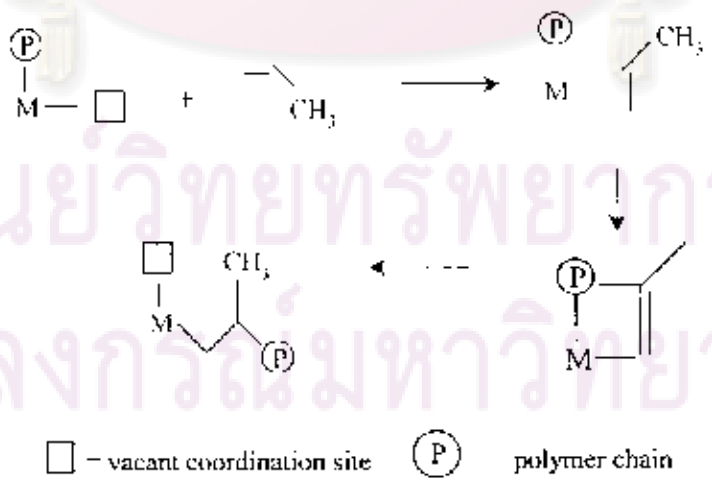

The trigger mechanism has been proposed for the polymerization of α-olefin with Ziegler-Natta catalysts [33]. In this mechanism, two monomers interact with one active catalytic center in the transition state. A second monomer is required to form a new complex with the existing catalyst-monomer complex, thus trigger a chain propagation step. No vacant site is involved in this model. The trigger mechanism has been used to explain the rate enhancement effect observed when ethylene is copolymerized with α-olefins.

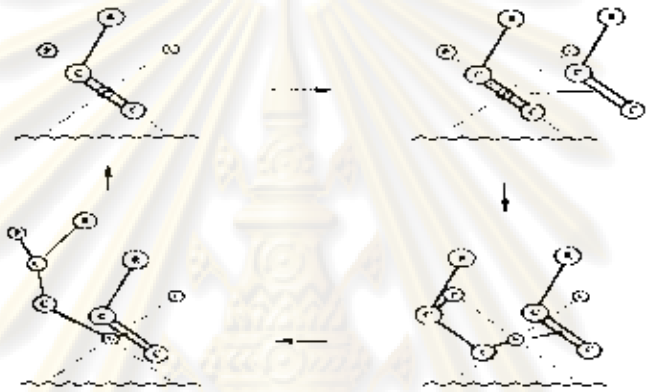

Figure 2.10 The propagation step according to the trigger mechanism [33].

After that, the propagation mechanism in polymerization shown in **Figure 2.11**

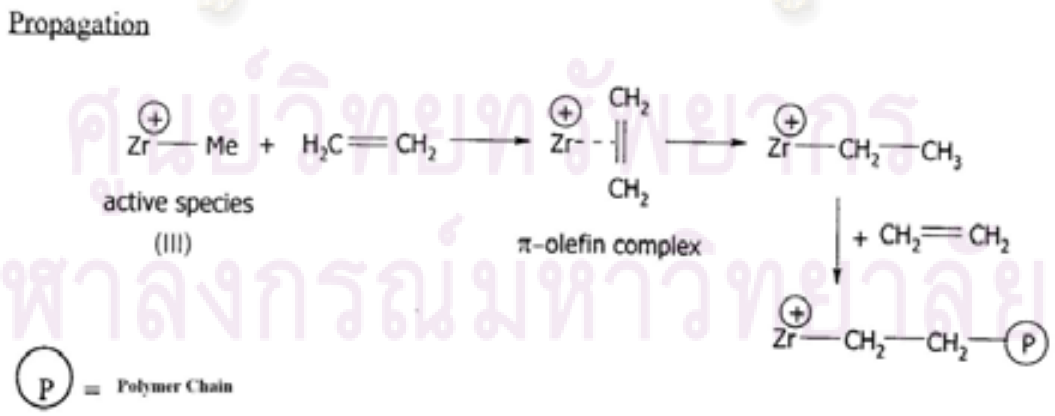

Figure 2.11 Propagation mechanism in polymerization

Finally, the termination of polymer chains can be formed by 1) chain transfer via β-H elimination, 2) chain transfer via β-Me elimination, 3) chain transfer to aluminum, 4) chain transfer to monomer, and 5) chain transfer to hydrogen (**Figure 2.12-2.16**) [43]. The first two transfer reactions form the polymer chains containing terminal double bonds.

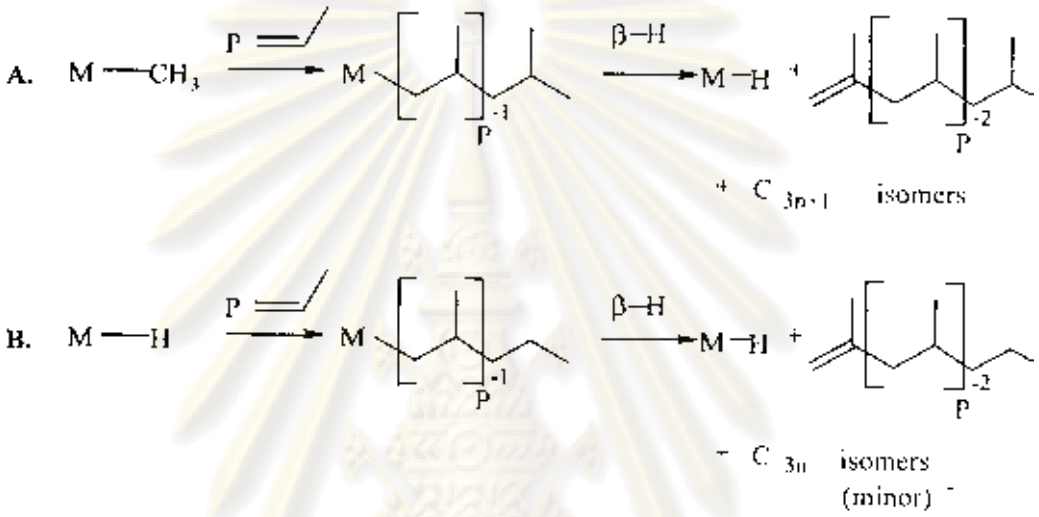

Figure 2.12 Chain transfer via β-H elimination [43]

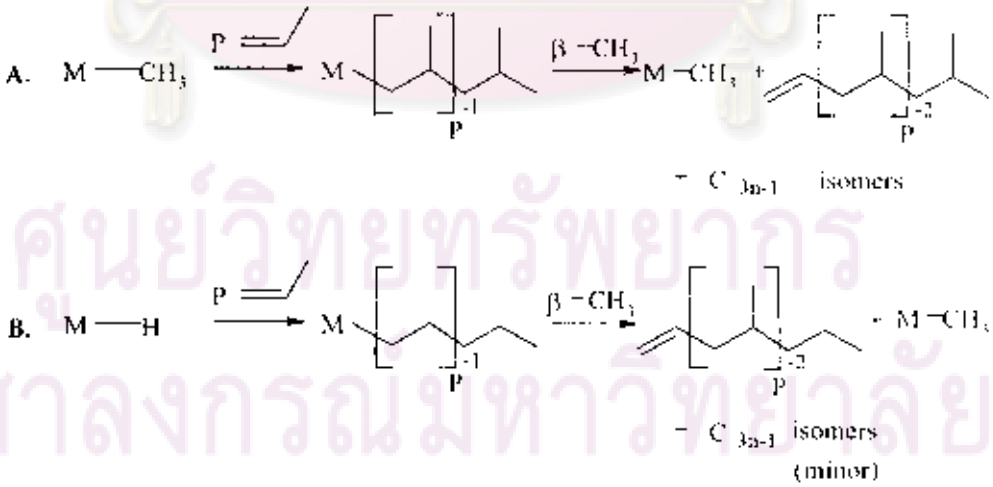

Figure 2.13 Chain transfer via β-CH_3 elimination [43]

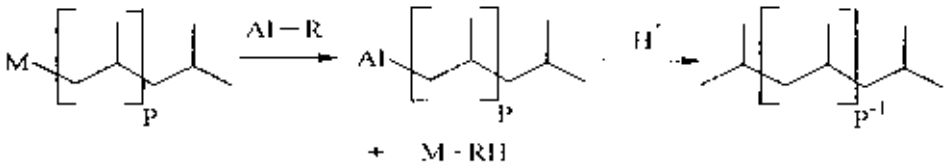

Figure 2.14 Chain transfer to aluminum [43]

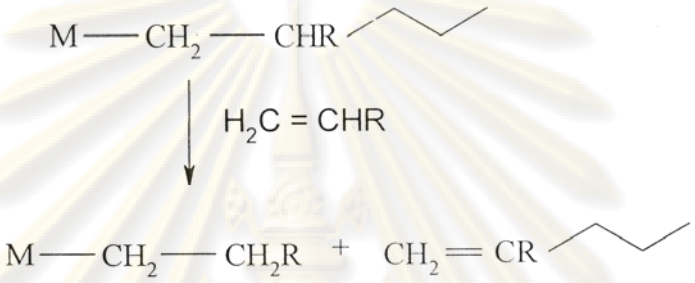

Figure 2.15 Chain transfer to monomer [43]

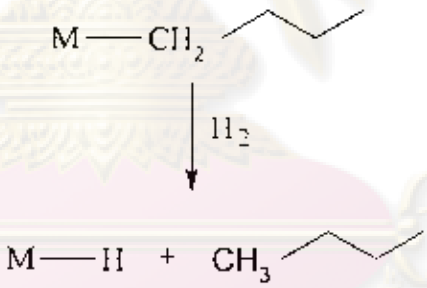

Figure 2.16 Chain transfer to hydrogen [43]

2.3.3 Cocatalysts

Metallocene catalysts have to be activated by a cocatalyst. The most common types of cocatalysts are alkylaluminums including methylaluminoxane (MAO), trimethylaluminum (TMA), triethylaluminum (TEA), triisobutylaluminum (TIBA) and cation forming agents such as $(C_6H_5)_3C^+(C_6F_5)_4B^-$ and $B(C_6F_5)_3$ [47].

Among these, MAO is a very effective cocatalyst for metallocene. However, due to the difficulties and costs involved in the synthesis of MAO, there has been considerable effort done to reduce or elimination the use of MAO. Due to difficulties in separation, most commercially available MAO contains a significant fraction of TMA (about 10-30%) [48]. This TMA in MAO could be substantially eliminated by toluene-evaporation at 25°C.

Indeed, the difficulties encountered to better understand the important factors for an efficient activation are mainly due to the poor knowledge of the MAO composition and structure. Several types of macromolecular arrangements, involving linear chains, monocycles and/or various three-dimensional structures have been successively postulated. These are shown in **Figure 2.17**. In recent work, a more detailed image of MAO was proposed as a cage molecule, with a general formula $Me_{6m}Al_{4m}O_{3m}$ (m equal to 3 or 4) [49].

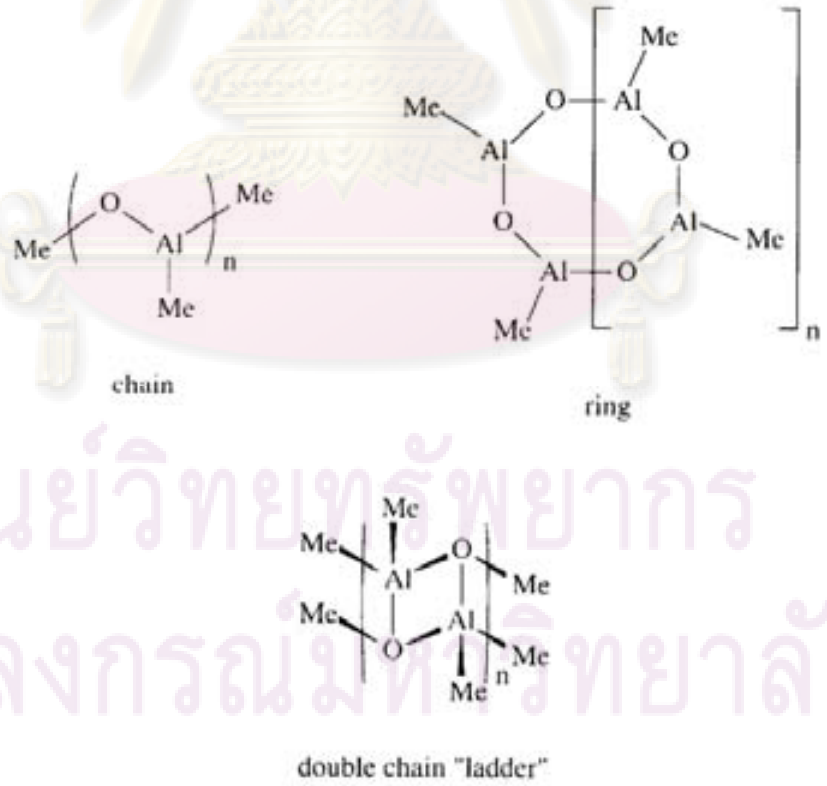

Figure 2.17 Early structure models for MAO [49]

In the case of rac-Et(Ind)$_2$ZrMe$_2$ as precursor, the extracted methyl ligands do not yield any modification in the structure and reactivity of the MAO counter-anion, thus allowing zirconium coordination site available for olefin that presented in **Figure 2.18** [50].

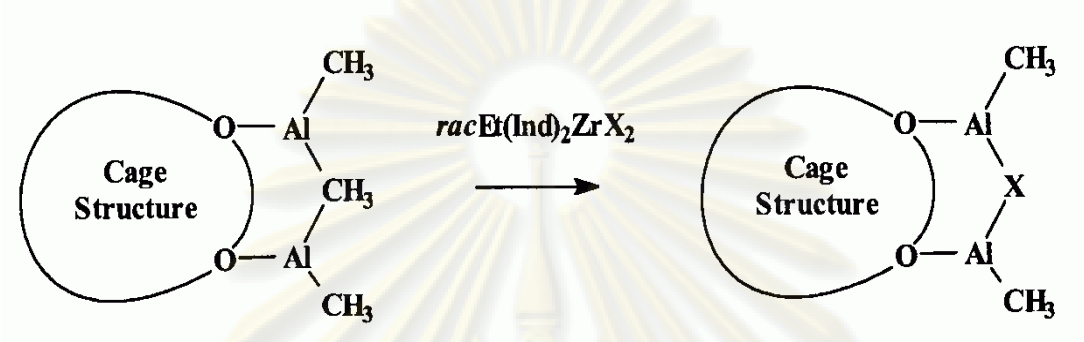

Figure 2.18 Representation of MAO showing the substitution of one bridging methyl group by X ligand extracted from racEt(Ind)$_2$ZrCl$_2$ (X=Cl, NMe$_2$, CH$_2$Ph) [50].

Cam and Giannini [51] investigated the role of TMA present in MAO by a direct analysis of Cp$_2$ZrCl$_2$/MAO solution in toluene-d$_8$ using ^{1}H-NMR. Their observation indicated that TMA might be the major alkylating agent and that MAO acted mainly as a polarization agent. However, in general it is believed that MAO is the key cocatalyst in polymerizations involving metallocene catalysts. The role of MAO included 1) alkylation of metallocene, thus forming catalyst active species, 2) scavenging impurities, 3) stabilizing the cationic center by ion-pair interaction and 4) preventing bimetallic deactivation of the active species.

The homogeneous metallocene catalyst cannot be activated by common trialkylaluminum only. However, Soga *et al*. [52] were able to produce polyethylene with modified homogeneous Cp$_2$ZrCl$_2$ activated by common trialkylaluminum in the presence of Si(CH$_3$)$_3$OH. Their results show that for an “optimum” yield aging of the catalyst and Si(CH$_3$)$_3$OH mixture for four hours is required. However, MWD of the produced polymers is bimodal although the polymers obtained in the presence of MAO have narrow MWD.

Ethylene/ -olefins copolymers with bimodal CCD were produced with homogeneous Cp_2ZrCl_2 with different cocatalysts such as MAO and mixture of TEA/borate or TIBA/borate [53]. It seemed that the active species generated with different cocatalysts have different activities and produce polymers with different molecular weights.

2.3.4 Catalyst Activity

The ethylene polymerization rate of the copolymerization reaction with the catalyst system SiO_2/MAO/rac-Me_2Si [2-Me-4-Ph-lnd]$_2ZrCl_2$ was studied by Fink *et al.* [54]. The temperature was varied from 40 to 57°C. Small amount of hexene in the reaction solution increased the polymerization rate. The extent of the "comonomer effect" depended on the polymerization temperature. At 57°C the maximum activity of the ethylene/hexene copolymerization was 8 times higher than the homopolymerization under the same conditions. At 40°C the highest reaction rate for the copolymerization is only 5 times higher than that for the ethylene homopolymerization. For the polymer properties of the ethylene/ -olefin copolymerization, the molecular weights of the polymers decreased with increasing comonomer incorporation. Ethylene/hexene copolymers produced by a metallocene catalyst also have the same melting point and glass transition temperature.

Series of ethylene copolymerization with 1-hexene or 1-hexadecene over four different siloxy-substituted ansa-metallocene/methylaluminoxane (MAO) catalyst systems were studied by Seppala *et al.* [55]. Metallocene catalysts rac-Et[2-(t-$BuMe_2SiO$)Ind]$_2ZrCl_2$ (1), rac-Et[l-(t-$BuMe_2SiO$)Ind]$_2ZrCl_2$ (2), rac-Et[2-(i-Pr_3SiO)Ind]$_2ZrCl_2$ (3) and rac-Et[l-(i-Pr_3SiO)Ind]$_2ZrCl_2$ (4) were used. The effects of minor changes in the catalyst structure, more precisely changes in the ligand substitution pattern were studied. They found that series of polymerization with siloxy-substituted bis(indenyl) ansa-metallocene are highly active catalyst precursors for ethylene-α-olefins copolymerizations. The comonomer response of all four catalyst precursors was good. Under the same conditions the order of copolymerization ability of the catalyst was rac-Et[2-(i-Pr_3SiO)Ind]$_2ZrCl_2$ >

rac-Et[2-(t-BuMe$_2$SiO)Ind]$_2$ZrCl$_2$ and rac-Et[l-(i-Pr$_3$SiO)Ind]$_2$ZrCl$_2$ > rac-Et[l-(t-BuMe$_2$SiO)Ind]$_2$ZrCl$_2$. These catalysts are able to produce high molecular weight copolymers.

2.3.5 Copolymerization

By adding a small amount of comonomer to the polymerization reactor, the final polymer characteristics can be dramatically changed. For example, the Unipol process for linear low density polyethylene (LLDPE) uses hexene and the British Petroleum process (BP) use 4-methylpentene to produce high-performance copolymers [56]. The comonomer can be affected the overall crystallinity, melting point, softening range, transparency and also structural, thermochemical, and rheological properties of the formed polymer. Copolymers can also be used to enhance mechanical properties by improving the miscibility in polymer blending [57].

Ethylene is copolymerized with α-olefin to produce polymers with lower densities. It is commonly observed that the addition of a comonomer generally increases the polymerization rate significantly. This comonomer effect is sometimes linked to the reduction of diffusion limitations by producing a lower crystallinity polymer or to the activation of catalytic sites by the comonomer. The polymer molecular weight often decreases with comonomer addition, possibly because of a transfer to comonomer reactions. Heterogeneous polymerization tends to be less sensitive to changes in the aluminum/transition metal ratio. Chain transfer to aluminum is also favored at high aluminum concentrations. This increase in chain transfer would presumably produce a lower molecular weight polymer. In addition, some researchers observed the decrease, and some observed no change in the molecular weight with increasing aluminum concentration [58].

The effect of polymerization conditions and molecular structure of the catalyst on ethylene/ -olefin copolymerization have been investigated extensively. Pietikainen and Seppala [59] investigated the effect of polymerization temperature on catalyst activity and viscosity average molecular weights for low molecular weight ethylene/propylene copolymers produced with homogeneous Cp$_2$ZrCl$_2$. Soga and Kaminaka [60] compared copolymerizations (ethylene/propylene, ethylene/1-hexene,

and propylene/l-hexene) with $Et(H_4Ind)_2ZrC1_2$ supported on SiO_2, Al_2O_3 or $MgCl_2$. Broadness of MWD was found to be related to the combination of support types and types of monomers. The effect of silica and magnesium supports on copolymerization characteristics was also investigated by Nowlin *et al.* [61]. Their results indicated that comonomer incorporation was significantly affected by the way that support was treated based on the reactivity ratio estimation calculated with simplified Finemann Ross method. However, it should be noted that Finemann Ross method could be misleading due to linear estimation of nonlinear system.

Copolymer based on ethylene with different incorporation of 1-hexene, 1-octene, and 1-decene were investigated by Quijada [62]. The type and the concentration of the comonomer in the feed do not have a strong influence on the catalytic activity of the system, but the presence of the comonomer increases the activity compared with that in the absence of it. From ^{13}C-NMR it was found that the size of the lateral chain influences the percentage of comonomer incorporated, 1-hexene being the highest one incorporated. The molecular weight of the copolymers obtained was found to be dependent on the comonomer concentration in the feed, showing that there is a transfer reaction with the comonomer. The polydispersity (Mw/Mn) of the copolymers is rather narrow and dependent on the concentration of the comonomer incorporation.

Soga *et al.* [63] noted that some metallocene catalysts produce two-different types of copolymers in terms of crystallinity. They copolymerized ethylene and 1-alkenes using 6 different catalysts such as Cp_2ZrCl_2, Cp_2TiCl_2, Cp_2HfCl_2, $Cp_2Zr(CH_3)_2$, $Et(Ind\ H_4)_2ZrCl_2$ and $i\text{-}Pr(Cp)(Flu)ZrCl_2$. Polymers with bimodal crystallinity distribution (as measured by TREF-GPC analysis) were produced with some catalytic systems. Only Cp_2TiCl_2-MAO and $Et(H_4Ind)_2ZrCl_2$-MAO produced polymers that have unimodal crystallinity distribution. The results seem to indicate that more than one active site type are present in some of these catalysts. However, it is also possible that unsteady-state polymerization conditions might have caused the broad distributions since the polymerization times were very short (5 minutes for most cases).

Marques *et al.* [64] investigated copolymerization of ethylene and 1-octene by using the homogeneous catalyst system based on $Et(Flu)_2ZrCl_2$/MAO. A study was performed to compare this system with that of Cp_2ZrCl_2/MAO. The influence of different support materials for the Cp_2ZrCl_2 was also evaluated, using silica, $MgCl_2$, and the zeolite sodic mordenite NaM. The copolymer produced by the $Et(Ind)_2ZrCl_2$/MAO system showed higher molecular weight and narrower molecular weight distribution, compared with that produced by Cp_2ZrCl_2/MAO system. Because of the extremely congested environment of the fluorenyl rings surrounding the transition metal, which hinders the beta hydrogen interaction, and therefore, the chain transference. Moreover, the most active catalyst was the one supported on SiO_2, whereas the zeolite sodic mordenite support resulted in a catalyst that produced copolymer with higher molecular weight and narrower molecular weight distribution. Both homogeneous catalytic systems showed the comonomer effect, considering that a significant increase was observed in the activity with the addition of a larger comonomer in the reaction medium.

The effect of different catalyst support treatments in the 1-hexene/ethylene copolymerization with supported metallocene catalyst was investigated by Soares *et al.* [65]. The catalysts in the study were supported catalysts containing SiO_2, commercial MAO supported on silica (SMAO) and MAO pretreated silica (MAO/silica) with Cp_2HfCl_2, $Et(Ind)_2HfCl_2$, Cp_2ZrCl_2 and $Et(Ind)_2ZrCl_2$. All the investigated supported catalysts showed good activities for the ethylene polymerization (400-3000 kg polymer/mol metal.h). Non-bridged catalysts tend to produce polymers with higher molecular weight when supported on to SMAO and narrow polydispersity. The polymer produced with Cp_2HfCl_2 supported on silica has only a single low crystallinity peak. On the other hand, Cp_2HfCl_2 supported on SMAO and MAO/silica produced ethylene/1-hexene copolymers having bimodal CCDs. For the case of Cp_2ZrCl_2 and $Et(Ind)_2ZrCl_2$, only unimodal CCDs were obtained. It seems that silica-MAO-metallocene and silica-metallocene site differ slightly in their ability to incorporate comonomer into the growing polymer chain, but not enough to form bimodals CCDs.

Soares *et al.* [66] studied copolymerization of ethylene and 1-hexene. It was carried out with different catalyst systems (homogeneous $Et(Ind)_2ZrCl_2$, supported $Et(Ind)_2ZrCl_2$ and in-situ supported $Et(Ind)_2ZrCl_2$). Supported $Et(Ind)_2ZrCl_2$: an $Et(Ind)_2ZrCl_2$ solution was supported on SMAO. It was used for polymerization of ethylene and 1-hexene. In-situ supported $Et(Ind)_2ZrCl_2$: an $Et(Ind)_2ZrCl_2$ solution was directly added to SMAO in the polymerization reactor, in the absence of soluble MAO. Homogeneous $Et(Ind)_2ZrCl_2$ showed higher catalytic activity than the corresponding supported and in-situ supported metallocene catalysts. The relative reactivity of 1-hexene increased in the following order: supported metallocene ≈ in-situ supported metallocene < homogeneous metallocene catalysts. The MWD and short chain branching distribution (SCBD) of the copolymer made with the in-situ supported metallocene were broader than those made with homogeneous and supported metallocene catalysts. They concluded that there are at least two different active species on the in-situ supported metallocene catalyst for the copolymerization of ethylene and 1-hexene.

Soares *et al.* [67] investigated copolymerization of ethylene and 1-hexene with different catalysts: homogeneous $Et(Ind)_2ZrCl_2$, Cp_2HfCl_2 and $[(C_5Me_4)SiMe_2N(tert\text{-}Bu)]TiCl_2$, the corresponding in-situ supported metallocene and combined in-situ supported metallocene catalyst (mixture of $Et(Ind)_2ZrCl_2$ and Cp_2HfCl_2 and mixture of $[(C_5Me_4)SiMe_2N(tert\text{-}Bu)]TiCl_2$. They studied properties of copolymers by using ^{13}C NMR, gel permeation chromatography (GPC) and crystallization analysis fractionation (CRYSTAF) and compared with the corresponding homogeneous metallocene. The in-situ supported metallocene produced polymers having different 1-hexene fractions, SCBD and MWD. It was also demonstrated that polymers with broader MWD and SCBD can be produced by combining two different in-situ supported metallocenes.

In addition, Soares *et al.* [52] studied copolymerization of ethylene and 1-hexene with an in-situ supported metallocene catalysts. Copolymer was produced with alkylaluminum activator and effect on MWD and SCBD was examined. They found that TMA exhibited the highest activity while TEA and TIBA had significantly lower activities. Molecular weight distributions of copolymers produced by using the

different activator types were unimodal and narrow, however, short chain branching distributions were very different. Each activator exhibited unique comonomer incorporation characteristics that can produce bimodal SCBD with the use of a single activator. They used individual and mixed activator system for controlling the SCBDs of the resulting copolymers while maintaining narrow MWDs.

2.4 Metallocene Catalysts

2.4.1 Olefin Polymerization with Metallocene Catalysts

The modern organometallic chemistry has begun when apply metallocene complexes with Group IV metals to new technologies and production of new materials. Metallocene compounds are becoming an important grade of catalysts for the synthesis of organic molecules and polymers. Metallocene catalysts are operated in all living industrial plants that are presently used for polyolefin manufacture revolutionize the technology for the production of these polymers [41].

Polyethylene's properties and the appropriate technology must be used to produce products which have the required properties by customer. This requires detailed knowledge and know-how of relationships among processing conditions, polymer structure and polymer properties. For catalytic polymerization processes the catalyst, mostly in combination with a cocatalyst, and the polymerization process are observed as the polymerization technology. This means that both the process and the catalyst are an integrated completion and must be well balanced in respect to each other [42]. The catalyst or catalyst system plays the key role, as polymerization behavior such activity, molecular mass regulation, copolymerization behavior, process control and polymer structure such molecular mass distribution, comonomer distribution, chain structure and polymer particle morphology such bulk density, particle size, particle distribution, in the choice of process and product properties [43]. The catalyst determines the polymerization behavior, the polymer structure and the polymer powder morphology in heterogeneous processes. The catalyst system must appropriate the polymerization process.

2.4.2 Catalyst Systems for Olefin Polymerization

In 1953 Karl Ziegler, who succeeded in polymerizing ethylene into high-density polyethylene (HDPE) at standard pressure and room temperature, discovered of catalysts based on titanium trichloride and diethylaluminum chloride as cocatalyst, at the Max-Planck-Institute in Mulheim. A little later, Natta, at the Polytechnical Institute of Milan, was able to indicate that an appropriate catalyst system was capable of polymerizing propene into semi-crystalline polypropene. Ziegler and Natta shared a Nobel Prize for Chemistry in 1963 for their work [33]. With this so-called Ziegler-Natta catalyst.

Ziegler-Natta catalyst has been widely used in olefin polymerization; the coordination polymerization allows the catalyst geometry around the metal center to control the polymer structure. In homogeneous polymerization, the ligand of a catalyst largely controls the geometry of an active metal center on which the polymerization reaction occurs. However, the conventional Ziegler-Natta catalysts the molecular structure of the polymers cannot be controlled well the molecular structure of the polymers because these catalysts have different nature types of catalytic sites.

Kaminsky discovered the metallocene catalyst system; it has proven to be a major breakthrough for the polyolefin industry. Metallocene catalysts show in opposite to conventional Ziegler-Natta catalytic systems, only one type of active site (single site catalyst), which produces polymers with a narrow molar mass distribution (M_w/M_n = 2). The molecular structure of the metallocene catalysts can be easily changed which allows control of the structure of polyolefin produced with these catalysts. Many metallocene are soluble in hydrocarbons or liquid propene. These properties allow one to predict accurately the properties of the resulting polyolefins by knowing the structure of the catalyst used during their manufacture and to control the resulting molar mass and distribution, comonomer content and tacticity by careful selection of the appropriate reactor conditions. In addition, their catalytic activity is 10-100 times higher than that of the classical Ziegler-Natta systems.

Metallocene, in combination with the conventional aluminum alkyl cocatalyst used in Ziegler systems, are indeed capable of polymerizing ethylene, but

only at a very low activity. Only with the discovery and application of methylaluminoxane (MAO) by Sinn et al., 1980, was it possible to enhance the activity, surprisingly, by a factor of 10,000. Therefore, MAO played a crucial part in the catalysis with metallocenes. Since this discovery of effective zirconocene-MAO catalyst systems for ethylene polymerization, development of the catalyst system has been conducted to achieve higher activity and to obtain higher molecular weight polyethylene. Modifications of metallocene ligand were investigated in non-bridged and bridged zirconocene catalysts [44].

The varying ligand of the metallocene can be changing the different microstructures and characteristics in polyolefin. By combining different olefins and cycloolefins with one another, the range of characteristics can be further broadened. The production of polyolefin with tailored microstructures and chemically uniform copolymers has not yet been achieved by conventional heterogeneous catalysts [33]. However, extensive research has been concerned towards metallocene catalyst studying modifications of the catalyst system, which leads to specific changes in catalytic activity and product characteristics [44]. The development of metallocene catalysts has not yet been complete, and studies are required to increase the understanding of several important factors which affect catalytic performance, such as transition metal-olefin interaction, metal-alkyl bond stability, influence of other ligands, and steric effects of the other ligands.

2.5 Heterogenous metallocene catalysts

The development of metallocene technologies has led to the synthesis of new polymers with different structures and properties to feed up the progressive demand of modern industry. According to the olefin polymerization, metallocences are crucial since they can control the properties of polyolefins. Metallocene catalysts are often used in the heterogeneous form based on the most existent technologies such as gas phase and slurry polymerization. Therefore, they are supported on an insoluble carrier prior to the polymerization. The reasons for the heterogenization of the metallocene are to slower the deactivation of the metallocene, employ less cocatalyst required,

protect the reactor fouling, control the polymer morphologies and fulfil the requirements of the commercial polymerization processes [69-70].

2.5.1 Supported metallocene catalysts method [69]

The main preparatory routes reported in the literature for metallocene immobilization on these supports can be classified according to three main methodologies, as follows:

1. The first method involves direct impregnation of metallocene on the support (modified by previous treatment or not). This can be done either (a) with mild impregnation conditions or (b) at high temperatures and long impregnation times (refined route).

2. The second method involves immobilization of MAO on the support followed by reaction with the metallocene compound. A modified version of this method involves the replacement of MAO by an aluminum alkyl.

3. The third method involves immobilization of aryl ligands on the support followed by addition of a metal salt such as zirconium halide; recently, titanium and neodymium halides have also been used to form the attached metallocene.

Method 1 involves physical mixing of metallocene and support, and it was one of the first preparatory routes used. In this method, the dry support is reacted first with the metallocene compound in a solvent such as toluene. The solid part is then recovered by filtration and washed with a hydrocarbon. The mixing temperature and the contact time are important parameters since they influence both the catalytic performances and the final properties of the polymer, as will be further discussed.

In 1991, Kaminaka and Soga used this impregnation method, at very mild conditions (room temperature and impregnation time, 10 min), to prepare and compare the performances of different supported systems. Later on, Kaminsky and Renner (1993) used a refined route (method 1b) for the preparation of silica-supported ansa-metallocene catalysts. This method involves direct reaction of metallocene with

SiO_2 at high temperature (T = 70 °C) and for a long period of time (16 h). The traces of the remaining highly active homogeneous catalyst were carefully extracted from the solid catalyst, to prevent the formation of low-melting and low-molecular-weight polypropylene.

The second and third methods have been mostly used for the preparation of silica-supported metallocenes. Silica is one of the most frequently used carriers, since it leads to good morphological features for polymer particles.

In method 2, silica is first pretreated with a small amount of MAO under mild conditions (room temperature, 30 min). After filtration and washing with toluene, the MAO-modified SiO_2 support is then mixed with the metallocene and treated as described in method 1. The supported zirconocenes obtained in this way can be activated by MAO [71-73] or by common alkylaluminum [60,74-75].

Method 3 deals with the synthesis of catalysts where metallocene ligands are chemically bonded to the support (mainly modified SiO_2). It involves four steps:

Step 1 is the modification of the silica surface by addition of compounds such as $SiCl_4$, $C_2H_2Br_4$, $SOCl_2$, or $MeSiCl_2$. Typical conditions are reaction in toluene at reflux for 48 h.

Step 2 is the reaction of modified SiO_2 with the lithium salt of the aryl derivatives to be immobilized (indenyllithium, cyclopentadienyllithium, fluorenyllithium, etc.). This step is generally achieved in THF at relatively low temperatures.

Step 3 is the treatment of the resulting aryl-grafted silica gel with a solution of butyllithium in hexane (at room temperature) to form new aryllithium derivatives.

Step 4 is the reaction of the latter system with zirconium, titanium [76] or neodymium [77] halides to yields supported metallocenes.

After each modification step, the silica is filtered and washed with large quantities of THF and finally evaporated to dryness under vacuum. These supported metallocenes can be used with either MAO or a common trialkylaluminum

as the cocatalyst. A typical catalyst preparation according to this procedure, as well as the structure of the species formed.

2.5.2 Supported metallocene with inorganic support

It has been reported that many inorganic supports such as carbon nanotube, SiO_2, Al_2O_3, $MgCl_2$ and TiO_2 [15-28] have been studied. The results from Ketloy *et al*. [14] showed that the obtained copolymers that used titania as a support exhibited a lower molecular weight than that of silica and silica-titania mixed oxide supports. In addition, titania can keep a lot of -OH groups at high temperature that have an important role in the metal complex anchoring and stabilization [78].

CHAPTER III

EXPERIMENTAL

3.1 Objectives of the Thesis

The objective of this research is to investigate the effect of titania having different phases as a support for metallocene catalyst for ethylene/α-olefin copolymerization on the polymerization activities and polymer characteristics.

3.2 Scopes of the Thesis

1. Characterization of the different titania supports using BET surface area , X-ray diffraction (XRD), scanning electron microscopy (SEM)
2. Preparation of supports by impregnation with dried MMAO (dMMAO)
3. Characterization of catalyst precursors using X-ray diffraction (XRD), energy-dispersive X-ray spectrometer (EDX), scanning electron microscopy (SEM), X-ray photoelectron spectroscopy (XPS) and inductively coupled plasma atomic emission spectrometer (ICP-AES)
4. Copolymerization of ethylene/α-olefin
5. Characterization of the obtained copolymer using scanning electron microscopy (SEM), differential scanning calorimeter (DSC) and ^{13}C-nuclear magnetic resonance (^{13}C-NMR)

3.3 Research Methodology

Research Methodology of flow diagram is show in **Figure 3.1**.

All reactions were conducted under argon atmosphere using Schlenk techniques and glove box.

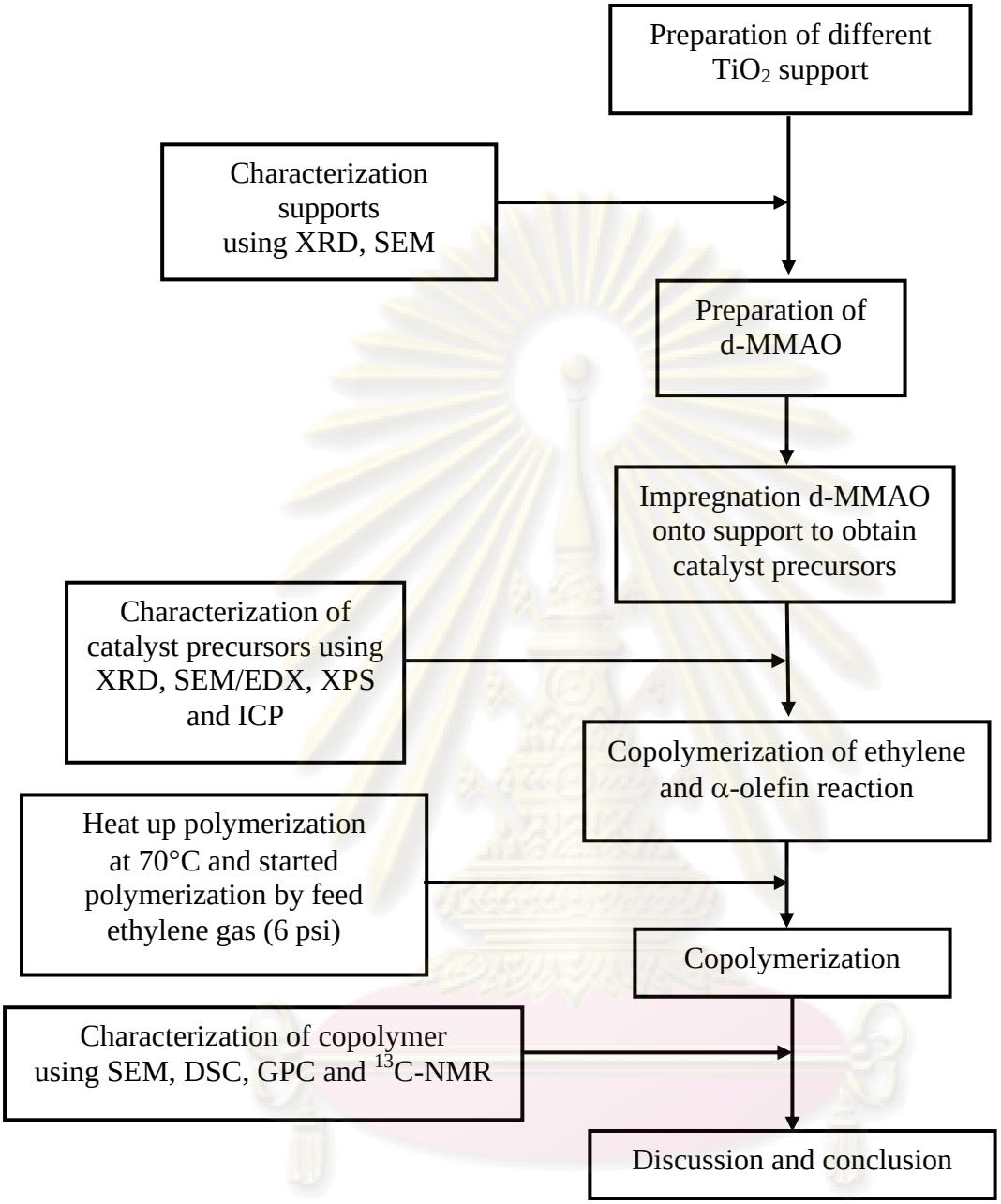

Figure 3.1 Flow diagram of research methodology

3.4 Experimental

3.4.1 Chemicals

The chemicals used in these experiments were analytical grade, but only major materials are specified as follows:

1. Ethylene gas (99.96%) was devoted from National Petrochemical Co., Ltd., Thailand and used as received.
2. 1-Hexene (97%) was purchased from Aldrich Chemical Company, Inc. and purified by distilling over sodium under argon atmosphere before use.
3. Hexane (95%) was donated from Shell (Public) Company, Inc. and purified by distilling over sodium under argon atmosphere before use.
4. Heptane (≥ 97%) was purchased from Fluka Chemie A.G. Switzerland and purified by distilling over sodium under argon atmosphere before used.
5. Toluene was devoted from EXXON Chemical Ltd., Thailand. This solvent was dried over dehydrated $CaCl_2$ and distilled over sodium/benzophenone under argon atmosphere before use.
6. Modified methylaluminoxane (MMAO) 1.86 M in toluene was donated from Tosoh Akso, Japan and used without further purification.
7. Titanium (IV) oxide micropowder (99.7%, pure anatase) was purchased from Aldrich Chemical Company, Inc. was vacuum heated at 400 °C for 6 hours.
8. Titanium (IV) oxide micropowder (99.5%, pure rutile) was purchased from Aldrich Chemical Company, Inc. was vacuum heated at 400 °C for 6 hours.
9. Zirconium (IV) propoxide 70 wt% solution in 1-propanol (d=0.803 g/ml) was supplied from Aldrich Chemical Company, Inc.
10. Hydrochloric acid (Fuming 36.7%) was supplied from Sigma and used as received.
11. Hydrofluoric acid (48%) was supplied from Merck and used as received.
12. Methanol (Commercial grade) was purchased from SR lab and used as received.
13. Sodium (99%) was purchased from Aldrich Chemical Company, Inc. and used as received.
14. Benzophenone (99%) was purchased from Fluka Chemie A.G. Switzerland and used as received.

15. Calciumhydride (99%) was purchased from Fluka Chemie A.G. Switzerland and used as received.

16. Ultra high purity argon gas (99.999%) was purchased from Thai Industrial Gas Co., Ltd., and further purified by passing through columns packed with molecular sieve 3A, BASF Catalyst R3-11G, sodium hydroxide (NaOH) and phosphorus pentaoxide (P_2O_5) to remove traces of oxygen and moisture.

3.4.2 Equipments

Due to the metallocene system is extremely sensitive to the oxygen and moisture. Thus, the special equipments were required to handle while the preparation and polymerization process. For example, glove box: equipped with the oxygen and moisture protection system was used to produce the inert atmosphere. Schlenk techniques (Vacuum and Purge with inert gas) are the others set of the equipment used to handle air-sensitive product.

3.4.2.1 Cooling system

The cooling system was in the solvent distillation in order to condense the freshly evaporated solvent.

3.4.2.2 Inert gas supply

The inert gas (argon) was passed through columns of BASF catalyst R3-11G as oxygen scavenger, molecular sieve 3×10^{-10} m to remove moisture. The BASF catalyst was regenerated by treatment with hydrogen at 300 ^{o}C overnight before flow the argon gas through all the above columns. The inert gas supply system is shown in **Figure 3.2.**

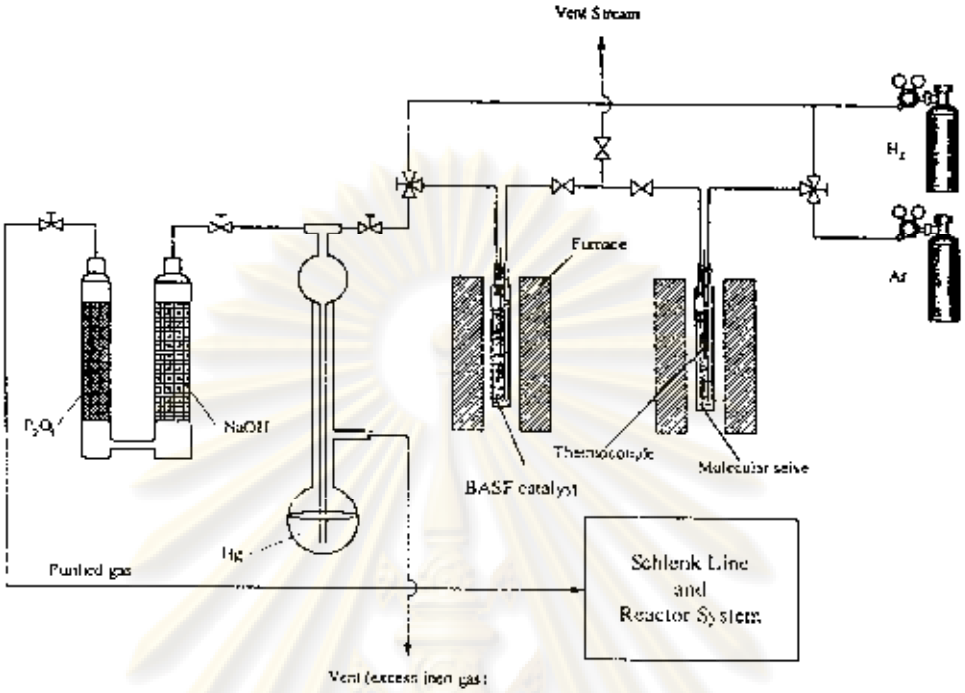

Figure 3.2 Inert gas supply system

3.4.2.3 Magnetic stirrer and heater

The magnetic stirrer and heater model RTC basis from IKA Labortechnik were used.

3.4.2.4 Reactor

A 100 ml glass flask connected with 3-ways valve was used as the copolymerization reactor for atmospheric pressure system and a 100 ml stainless steel autoclave was used as the copolymerization reactor for high pressure systems.

3.4.2.5 Schlenk line

Schlenk line consists of vacuum and argon lines. The vacuum line was equipped with the solvent trap and vacuum pump, respectively. The argon line was connected with the trap and the mercury bubbler that was a manometer tube and contains enough mercury to provide a seal from the atmosphere when argon line was evacuated. The Schlenk line was shown in **Figure 3.3.**

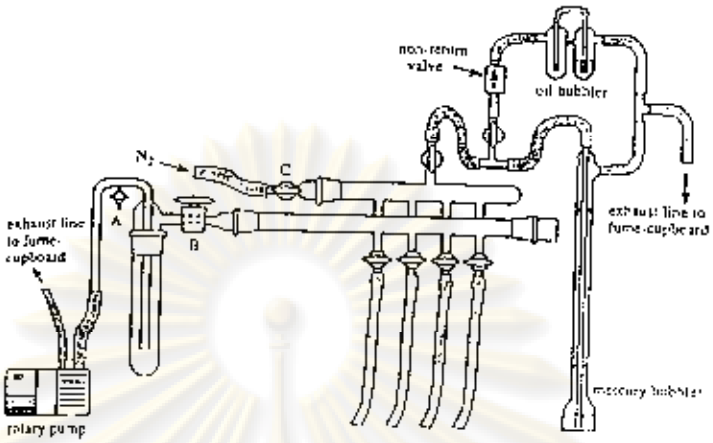

Figure 3.3 Schlenk line

3.4.2.6 Schlenk tube

A tube with a ground glass joint and side arm, which was three-way glass valve as shown in **Figure 3.4.** Sizes of Schlenk tubes were 50, 100 and 200 ml used to prepare catalyst and store materials which were sensitive to oxygen and moisture.

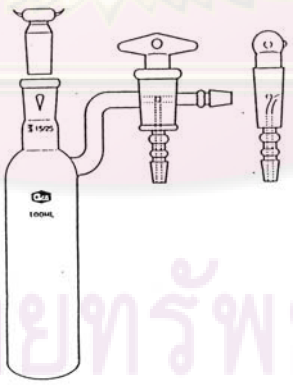

Figure 3.4 Schlenk tube

3.4.2.7 Vacuum pump

The vacuum pump model 195 from Labconco Corporation was used. A pressure of 10^{-1} to 10^{-3} mmHg was adequate for the vacuum supply to the vacuum line in the Schlenk line.

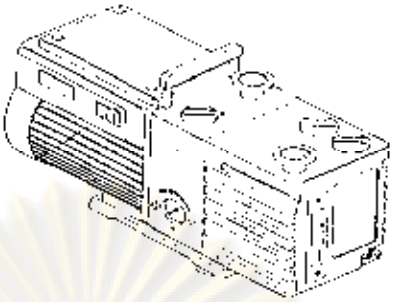

Figure 3.5 Vacuum pump

3.4.2.8 Polymerization line

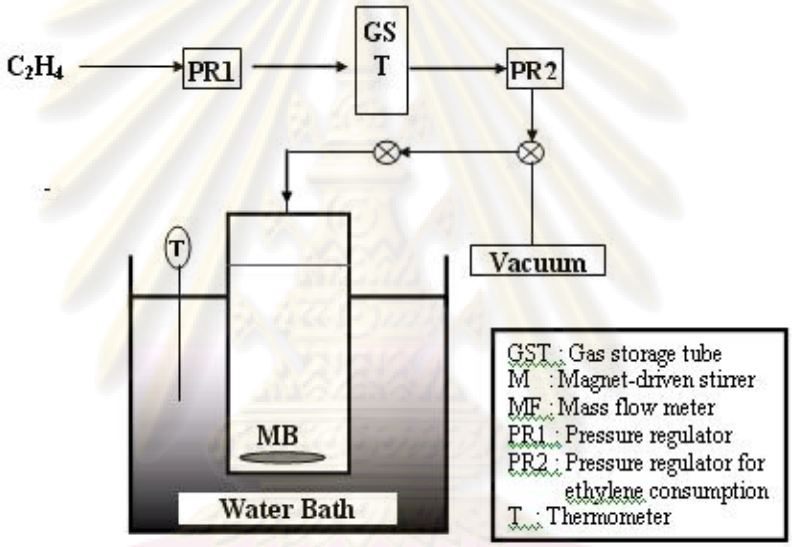

Figure 3.6 Diagram of system in slurry phase polymerization

3.4.3 Supporting Procedure

3.4.3.1 Preparation of dried-MMAO (dMMAO)

Removal of TMA from MMAO was carried out according to the reported procedure [79]. The toluene solution of MMAO was dried under vacuum for 6 hours at room temperature to evaporate the solvent, TMA, and Al(*i*Bu)$_3$ (TIBA). Then, continue to dissolve with 100 ml of heptane and the solution was evaporated under vacuum to remove the remaining TMA and TIBA. This procedure was repeated 6-8 times and the white powder of dried MMAO (dMMAO) was obtained.

3.4.3.2 Preparation of supported dMMAO (catalyst precursor)

The TiO_2 support was reacted with the desired amount of dMMAO in 20 ml of toluene at room temperature for 30 min. The solvent was then removed from the mixture by evacuated. This procedure was done twice with toluene (20 ml x 2) and 3 times with hexane (20 ml x 3). Then, the solid part was dried under vacuum at room temperature. The white powder of supported cocatalyst (dMMAO/support) was then obtained.

3.4.4 Ethylene/α-olefin Polymerization Procedures

The ethylene/α-olefin copolymerization reaction was carried out in a 100 ml semi-batch stainless steel autoclave reactor equipped with magnetic stirrer. In the glove box, the desired amounts of *rac*-Et[Ind]$_2$ZrCl$_2$ and TMA were mixed and stirred for 5 min for aging. Then, toluene (to make a total volume of 30 ml) and 100 mg of dMMAO/support were introduced into the reactor. After that, the mixture of *rac*-Et[Ind]$_2$ZrCl$_2$ and TMA were injected into the reactor. The reactor was frozen in liquid nitrogen to stop reaction and then 0.018 mol of α-olefin was injected into the reactor. The reactor was evacuated to remove argon. Then, it was heated up to polymerization temperature (70 ^{o}C) and the polymerization was started by feeding ethylene gas (total pressure 50 psi in the reactor) until the consumption of ethylene 0.018 mol (6 psi was observed from the pressure gauge) was reached. The reaction of polymerization was completely terminated by addition of acidic methanol. The time of reaction was recorded for purpose of calculating the activity. The precipitated polymer was washed with methanol and dried at room temperature.

3.4.5 Characterization of supports and catalyst precursor

3.4.5.1 N_2 physisorption

Measurement of BET surface area, average pore diameter and pore size distribution of MCM-41 support were determined by N_2 physisorption using a Micromeritics ASAP 2000 automated system.

3.4.5.2 X-ray diffraction (XRD)

XRD was performed to determine the bulk crystalline phases of sample. It was conducted using a SIEMENS D-5000 X-ray diffractometer with CuK_{α}(λ = 1.54439×10^{-10} m). The spectra were scanned at a rate 2.4 degree/min in the range 2θ = 20-80 degrees.

3.4.5.3 Thermal gravimetric analysis (TGA)

TGA was performed to determine the interaction force of the supported dMMAO. It was conducted using TA Instruments SDT Q 600 analyzer. The samples of 10-20 mg and a temperature ramping from 25 to 600 °C at 2 °C /min were used in the operation. The carrier gas was N_2 UHP.

3.4.5.4 Scanning electron microscopy (SEM) and energy dispersive X-ray spectroscopy (EDX)

SEM and EDX were used to determine the morphologies and elemental distribution throughout the sample granules, respectively. The SEM of JEOL mode JSM-6400 was applied. The EDX was performed using Link Isis series 300 program.

3.4.5.5 Inductively coupled plasma atomic emission spectrometer (ICP-AES)

ICP-AES using Perkin Elmer model PLASMA-1000 at Scientific Technological Research Equipment Center, Chulalongkorn University will be employed to investigate the content of aluminium and titanium of catalyst precursor. The catalyst precursor will be dissolved by hydrofluoric acid (48%) 5 ml. The mixture will be stirred and heated at 50 °C over night. After the catalyst precursor will be completely dissolved, the solution will be diluted to a volume of 100 ml.

3.4.5.6 X-ray photoelectron spectroscopy (XPS)

The XPS analysis will be performed using an AMICUS photoelectron spectrometer ESCA-3400 equip with an Mg Kα X-ray as primary excitation and

KRATOS VISION2 software. XPS elemental spectra will be acquired with 0.1 eV energy step as a pass energy of 75 kV. The C 1s line will be taken as an internal standard at 285.0 eV.

3.4.5.7 Transmission electron microscopy (TEM)

TEM was used to determine the morphologies and crystallite size of TiO2 supports. The sample was dispersed in ethanol before using TEM (JEOL JEM-2010) at Scientific Technological Research Equipment Center, Chulalongkorn University for microstructural characterization.

3.4.6 Characterization Method of Polymer

3.4.6.1 Differential scanning calorimetry (DSC)

The melting temperature of polymer products was determined with thermal analysis measurement. It was performed using a TA instrument 2910. The DSC measurements reported here were recorded during the second heating/cooling cycle with the rate of 20 °C min^{-1}. This procedure ensured that the previous thermal history was erased and provided comparable conditions for all samples. Approximately 10 mg of sample was used for each DSC measurement.

3.4.6.2 ^{13}C NMR spectroscopy (^{13}C NMR)

^{13}C NMR spectroscopy was used to determine the α-olefin incorporation and copolymer microstructure. Chemical shift were referenced internally to the benzene-d6 and calculated according to the method described by Randall [80]. Sample solution was prepared by dissolving 50 mg of copolymer in 1,2,4-trichlorobenzene and benzene-d6. ^{13}C NMR spectra were taken at 60 °C using BRUKER A400 operating at 100 MHz with an acquisition time of 1.5 s and a delay time of 4 s.

CHAPTER IV

RESULTS AND DISCUSSIONS

The purpose of this study is to investigate effects of different phases of titania supports on the catalyst activity and properties of copolymers during ethylene/α-olefin polymerization with the zirconocene catalyst. The supports and supported-dMMAO (catalyst precursors) were also investigated to make better understanding about polymerization results.

4.1 Characterization of supports and supported dMMAO

4.1.1 Characterization of supports with N_2 physisorption

The surface areas, average pore diameter and pore volume for all different supports, such as TiO_2 (A), TiO_2 (R) and TiO_2 (M) are listed in **Table 4.1**. It showed slightly larger surface area of TiO_2 (A) than that of TiO_2 (R) and TiO_2 (M).

Table 4.1 Characteristic of different TiO_2 supports

Types of support	Surface area (m^2g^{-1})	Crystallite size [a] (μm)	Average pore diameter (nm)	Pore volume ($cm^3\ g^{-1}$)
TiO_2 (A)	10.6	0.5-3	8.12	0.021519
TiO_2 (M)	6.2	3-7	6.71	0.011064
TiO_2 (R)	3.5	2-8	4.98	0.004938

[a] Based on TEM measurement

4.1.2 Characterization of supports with X-ray diffraction (XRD)

The various titania supports with different phases were characterized before and after impregnation with dMMAO. The XRD patterns of supports with different phases are shown in **Figure 4.1**. The characteristic peaks for the anatase form of TiO_2 (A) at 25° (major), 38°, 48°, 55°, and 63° and the rutile form of TiO_2 (R) at 27° (major), 36°, 41°, and 54° and the mixed form of TiO_2 (M) at 25° and 27° (major), 36°, 38°, 41°, 48°, 54°, 55°, and 63° were observed. After impregnation with dMMAO the XRD patterns for both samples exhibited the similar pattern. No peaks of dMMAO were detected. This was suggested that the dMMAO was in the highly dispersed form on the TiO_2 supports.

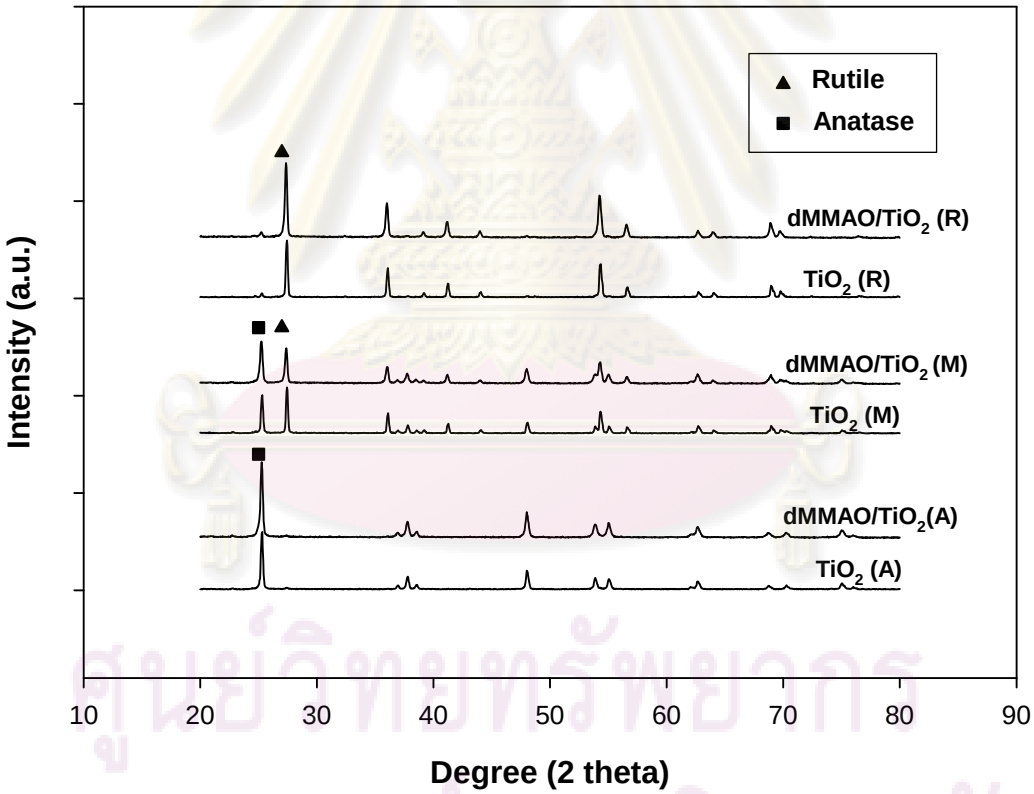

Figure 4.1 XRD patterns of different TiO_2 supports before and after impregnation with dMMAO

4.1.3 Characterization of supports with X-ray photoelectron spectroscopy (XPS)

The binding energy of Al_{2p} core-level of $[Al]_{dMMAO}$ was measured by XPS and listed in **Table 4.2** indicating the BE of 74.5-75.1 eV. These values were also in accordance with the MMAO present on the MCM-41, SiO_2 and TiO_2 support, as reported by Bunchongturakarn *et al*. [12], Ketloy *et al*. [14], Hagimoto *et al*. [79], Jiamwijitkul *et al*. [80] and Jongsomjit *et al*. [81]. Such results suggested that no significant change in the oxidation state of $[Al]_{dMMAO}$ occurred upon the various supports employed. As a matter of fact, the changes of the surface species was not the cause of the differences in polymerization activities observed on various supports. The other one for XPS is to characterized the content of $[Al]_{dMMAO}$ on TiO_2 supports compare with SEM/EDX and ICP/AES, the results were shown in **Table 4.2**.

4.1.4 Characterization of supports and supported dMMAO with scanning electron microscope (SEM) and energy dispersive X-ray spectroscopy (EDX)

SEM and EDX were performed to determine the content of $[Al]_{dMMAO}$ and the elemental distributions and the morphologies of supports. The SEM micrographs and EDX mapping for the dMMAO/TiO_2 samples are shown in **Figure 4.2**. All samples apparently exhibited the similar morphologies. It can be observed that the dMMAO was well distributed all over the TiO_2 granules as seen by the EDX mapping. After impregnation of supports with dMMAO, the $[Al]_{dMMAO}$ content was measured using EDX. The amounts of $[Al]_{dMMAO}$ in various TiO_2 supports are listed in **Table 4.2**.

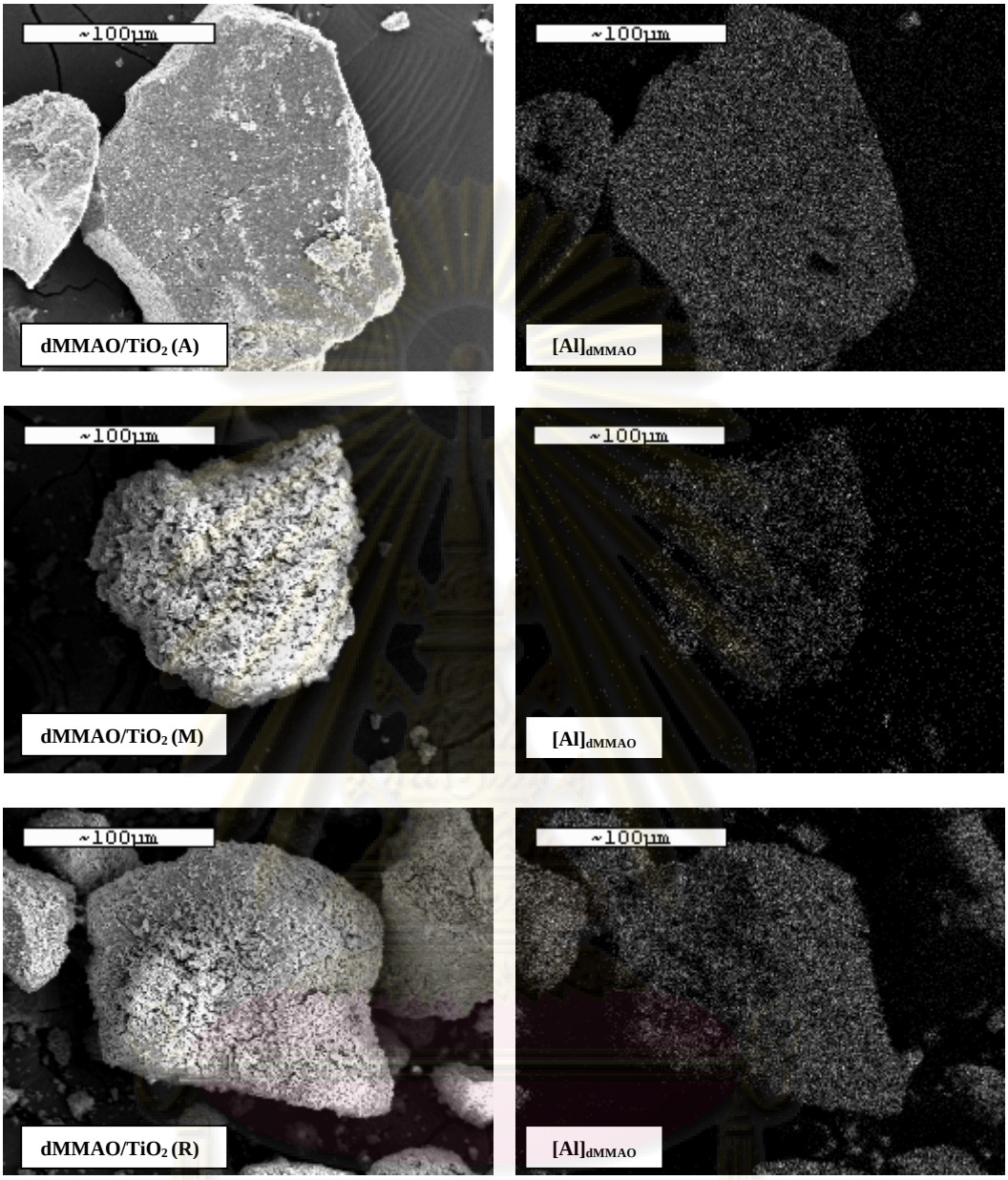

Figure 4.2 SEM micrographs and EDX mapping for different dMMAO/TiO_2 supports

4.1.5 Characterization of supports and supported dMMAO with Inductively coupled plasma atomic emission spectrometer (ICP-AES)

ICP-AES was used to determine the amount of $[Al]_{dMMAO}$ on the various TiO_2 supports compare with XPS and SEM/EDX. The results were shown in **Table 4.2**.

Table 4.2 Elemental analysis of Al and Ti obtained from XPS, EDX and ICP, and decomposition temperature

Types of catalyst precursor	Ratio of $[Al]_{dMMAO}/[Ti]_{support}$			BE (eV)[a] for Al_{2p}	T_{d5}[b] (^oC)
	XPS	EDX	ICP		
dMMAO/TiO_2 (A)	127.3 (43.7)	1.4 (22.8)	0.8 (16.8)	74.5	173
dMMAO/TiO_2 (M)	110.8 (43.6)	1.0 (19.1)	0.9 (18.0)	75.1	171
dMMAO/TiO_2 (R)	252.4 (43.9)	1.3 (22.0)	1.0 (19.1)	75.0	134

[a] Obtained from XPS [b] Obtained from TGA

( ) is %wt of aluminium in catalyst precursors

Results showed that the amounts of $[Al]_{dMMAO}$ at surface of all TiO_2 supports from XPS is the highest among those obtained by other techniques. The depth from the surface of characterization by different method was XPS ~ 1-3 nm, EDX ~ 1μm and ICP is bulk technique. This was suggested that most of $[Al]_{dMMAO}$ was located at the outer or external surfaces of TiO_2 supports.

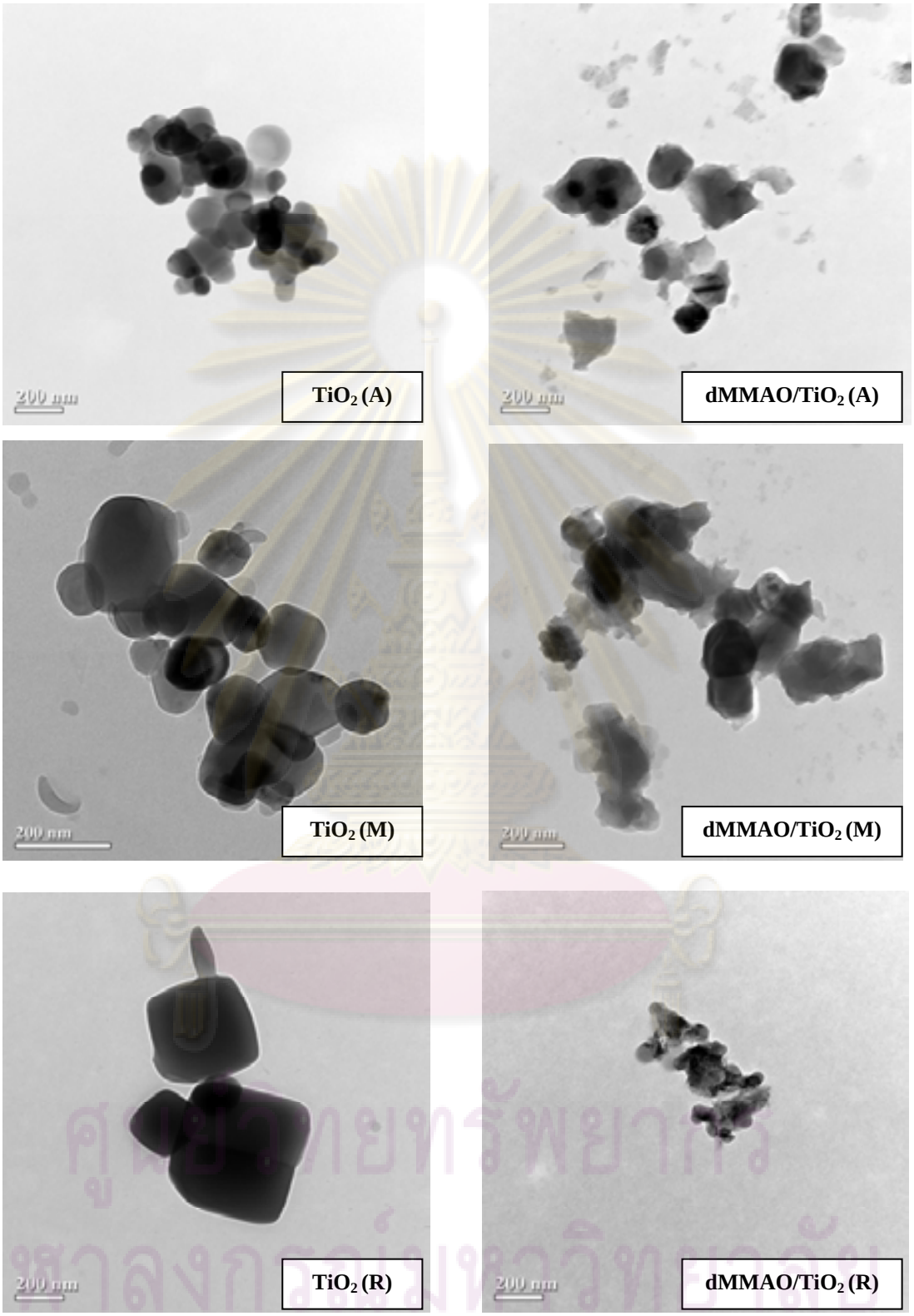

Fig. 4.3 TEM micrographs of different TiO_2 supports before and after impregnation with dMMAO

4.1.6 Characterization of supports and supported dMMAO with Transmission electron microscopy (TEM)

In order to determine the dispersion of TiO_2 before and after dMMAO impregnation, a more powerful technique, such as TEM was applied to all samples. The TEM micrographs of all TiO_2 supports before and after impregnation with dMMAO are shown in **Figure 4.3**. It indicated that crystallite sizes of TiO_2 after impregnation appeared to be smaller than those before impregnation. It was suggested that the fragmentation of TiO_2 crystals occurred after the dMMAO impregnation. The particle size of catalyst precursor in the rutile phase is the amallest and bunchy, mixed phase is dispersed more than rutile and anatase has the most dispersion.

4.1.7 Characterization of supports and supported dMMAO with Thermo gravimetric analysis (TGA)

In this study, dMMAO was dispersed by impregnation onto the various supports. The degree of interaction between the support and the cocatalyst (dMMAO) can be determined by the TGA measurement. The TGA provide information on the degree of interaction for the dMMAO bound to the support in terms of weight loss and removal temperature. The TGA profiles of $[Al]_{dMMAO}$ on various supports are shown in **Figure 4.4** indicating the similar profiles for various supports. The species having strong interaction with the support was removed at 997 °C. It was observed that the weight loss of $[Al]_{dMMAO}$ present on TiO_2 (A), TiO_2 (M) and TiO_2 (R) supports were in the order of 16.15% < 17.32% < 21.42%, respectively. This indicated that $[Al]_{dMMAO}$ present on TiO_2 (A) support had the strongest interaction > TiO_2 (M) > TiO_2 (R) support. The T_{d5} of the various supports were listed on **Table 4.2**. Considering the T_{d5} of TiO_2 (R) is the lowest probably due to the $[Al]_{dMMAO}/[Ti]_{support}$ of TiO_2 (R) is present on the surface more than that in the pore, Al can be extricated from TiO_2 (R) easier than the others.

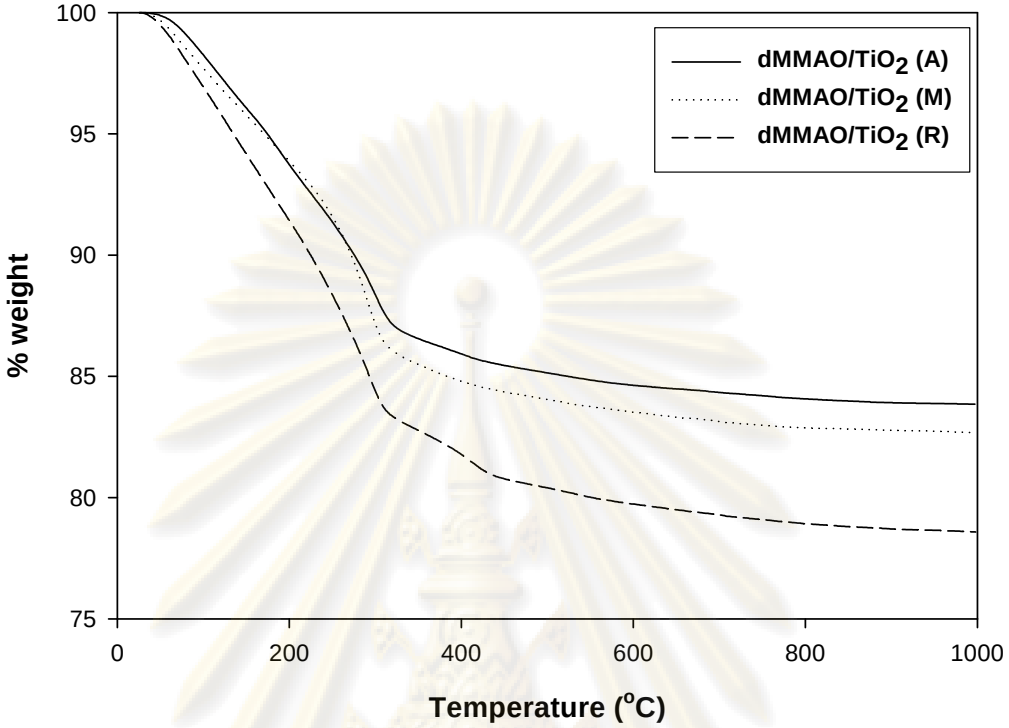

Figure 4.4 TGA profiles of $[Al]_{dMMAO}$ on different TiO_2 supports

4.2 Characteristic and catalytic properties of ethylene/1-hexene copolymerization

The various supports [TiO_2 (A), TiO_2 (M) and TiO_2 (R)] after impregnation with dMMAO [dMMAO/TiO_2 (A), dMMAO/TiO_2 (M) and dMMAO/ TiO_2 (R)] were used and investigated for catalytic activities. The ethylene/1-hexene copolymerization via various supported dMMAO with (*rac*-Et[Ind]$_2$ZrCl$_2$) was performed in order to determine the characteristic and catalytic properties of copolymer influenced by the various supports. Dried modified methylaluminoxane (dMMAO) was used as cocatalyst which all supports were fixed the $[Al]_{dMMAO}/[Zr]_{cat}$ ratios of 1135. The copolymerization were performed in toluene at 70 °C feeding 0.018 mol of ethylene gas (6 psi was observed from the pressure gauge), pressure in reactor = 50 psi, 0.018 ml of 1-hexene and zirconium concentration 10×10^{-5} M with total solution volume of 30 ml.

4.2.1 The effect of various supports on the catalytic activity

The catalytic activities via various supports and the homogeneous system are listed in **Table 4.3**.

Table 4.3 Polymerization activities for different TiO_2 supports

Types of support	Time[a] (s)	Polymer yield[b] (g)	Catalytic activity [kg polymer (mol Zr h)$^{-1}$]
Homogeneous	126	1.36	25,905
TiO_2 (A)	138	0.98	17,107
TiO_2 (M)	193	0.77	9,594
TiO_2 (R)	144	0.79	13,162

[a] The polymer yield was fixed [limited by ethylene fed and 1-hexene used (0.018 mole equally)].

[b] Activities were measured at polymerization temperature of 70 °C, [Ethylene] = 0.018 mole, $[Al]_{dMMAO}$ /$[Zr]_{cat}$ = 1135, $[Al]_{TMA}$ /$[Zr]_{cat}$ = 2500, in toluene with total volume = 30 ml and $[Zr]_{cat} = 5\times10^{-5}$ M.

For comparative studies, the polymerization activities towards copolymerization of ethylene/1-hexene upon the presence of different supports were measured. During polymerization, we kept the $[Al]_{dMMAO}/[Zr]_{cat}$ ratio being constant at 1135 by fixing the amount of catalyst and varying the amount of dMMAO/TiO_2 used based on the amount of $[Al]_{dMMAO}$ present as measured by ICP. Thus, increased activity can be attributed to more available active sites rather than more amounts of $[Al]_{dMMAO}$ being present. The polymerization activities of the homogeneous and the heterogeneous systems are listed in **Table 4.3**. The polymerization activities were in the order of homogeneous system > TiO_2 (A) > TiO_2 (R) > TiO_2 (M). As known, the activities of the supported system were apparently lower than homogeneous one due to supporting effect [26,82-83]. Among the supported systems, the polymerization activity obtained from the TiO_2 (A) was the highest. This was presumably due to the

more highly dispersion of the catalyst precursor resulting in high activity observed. Because of the constant ratio of $[Al]_{dMMAO}/[Zr]_{cat}$, the interaction between the $[Al]_{dMMAO}$ and TiO_2 supports was also important to consider. The connection of supports and dMMAO occurred via the $O_{support}$–$Al_{cocatalyst}$ linkage [84]. In particular, the TGA can only provide useful information on the degree of interactions for the dMMAO bound to the TiO_2 supports in terms of the weight loss and removal temperature. The suitable interaction can result in it being more suitable for the dMMAO bound to the TiO_2 supports to react with Zr-complex during activation process, leading to higher catalytic activity for polymerization. The weaker interaction can result in higher weight loss and the leaching of the active site leading to the lower catalytic activity for polymerization, as seen for TiO_2 (R) support compared to the TiO_2 (A) support. The TGA profiles of all dMMAO/TiO_2 samples are shown in **Figure 4.4** to possibly prove the interaction between $[Al]_{dMMAO}$ and TiO_2 supports. The weight loss of $[Al]_{dMMAO}$ present on TiO_2 supports was in the order of TiO_2 (R)(21.42%) > TiO_2 (M)(17.32%) > TiO_2 (A)(16.15%). The other explanation for catalytic activity between the different support TiO_2 (M) and TiO_2 (R) is about content of $[Al]_{dMMAO}$ on the TiO_2 support. From SEM/EDX and ICP/AES results, it can be observed that the high catalytic activity was probably due to the high content of $[Al]_{dMMAO}$.

4.2.2 The effect of various supports on the melting temperatures of copolymers

The melting temperatures (T_m) of copolymer were evaluated by the differential scanning calorimeter (DSC) are shown in **Table 4.4**. DSC curves of the copolymer are also shown in Appendix C. The melting temperatures (T_m) obtained from the DSC measurement is shown in **Table 4.4**, which trend to decrease with more insertion of 1-hexene due to decreased crystallinity.

Table 4.4 Triad distribution of LLDPE/TiO_2 copolymer obtained from ^{13}C NMR analysis and thermal property from DSC measurement

Type of supports	T_m (^oC)	EEE	HEE + EEH	HEH	EHE	EHH + HHE	HHH	1-Hexene incorporation (%)
TiO_2 (A)	83.3	0.67	0.15	0	0	0	0.18	18.45
TiO_2 (M)	89.5	0.63	0.14	0	0.02	0	0.20	22.51
TiO_2 (R)	82.8	0.48	0.18	0	0.10	0.24	0	33.21

E refers to ethylene monomer and H refers to 1-Hexene comonomer

4.2.3 The effect of various supports on the incorporation of copolymers

The quantitative analysis of triad distribution for all copolymers was conducted on the basis assignment of the ^{13}C NMR spectra of ethylene/1-hexene copolymer and calculated according to the method of Randall [85]. The characteristics of ^{13}C NMR spectra (as shown in appendix E) for all copolymers were similar indicating the copolymer of ethylene/1-hexene. The triad distribution of all polymers is shown in **Table 4.4**. It was found that ethylene incorporation in all systems gave copolymers with similar triad distribution. Based on calculations described by Galland [86], the triad distributions of ethylene (E) and 1-hexene (H) incorporation are listed in **Table 4.4**. It indicated that all LLDPE/TiO_2 supports obtained from different TiO_2 supports were random copolymer having different degrees of 1-hexene incorporation. From the TEM micrograph, TiO_2 (R) is the smallest particle size that brings to the highest surface area and makes the highest 1-hexene insertion. From the XPS data, $[Al]_{dMMAO}/[Ti]_{support}$ of TiO_2 (R) is the highest, that make the $[Al]_{dMMAO}$ is on the outer surface more than pore resulting the insertion of comonomer is easily than the others phases. In order to give a better understanding, a conceptual model for dispersion of active sites on TiO_2 surface is illustrated as shown in **Figure 4.5**. For the melting temperature, TiO_2 (R) is the lowest and TiO_2 (M) is the highest.

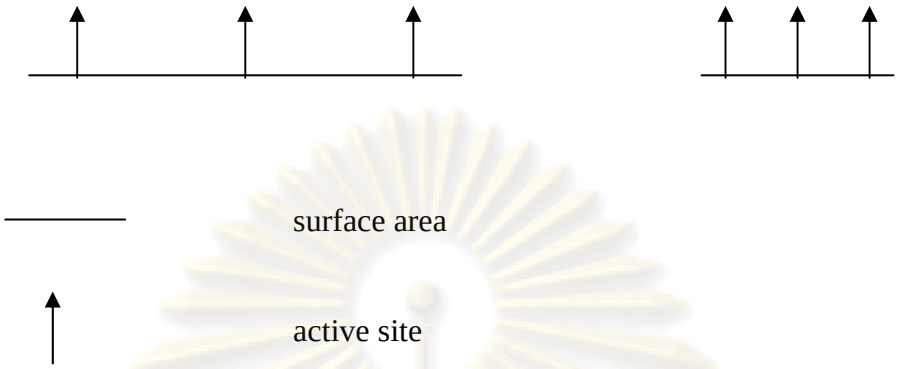

Figure 4.5 Conceptual models for dispersion of active sites on TiO_2 surface

4.2.4 The effect of various supports on the morphology of copolymers

In order to study the morphologies and TiO_2 distribution inside the polymer matrix of LLDPE/TiO_2 copolymers, SEM/EDX was performed. The SEM micrographs and EDX mapping for Ti of all samples are shown in **Figure 4.6**. There was no significant change in morphologies for all samples upon the different TiO_2 supports employed. Based on the EDX mapping, it showed good distribution of the TiO_2 supports inside the polymer matrix.

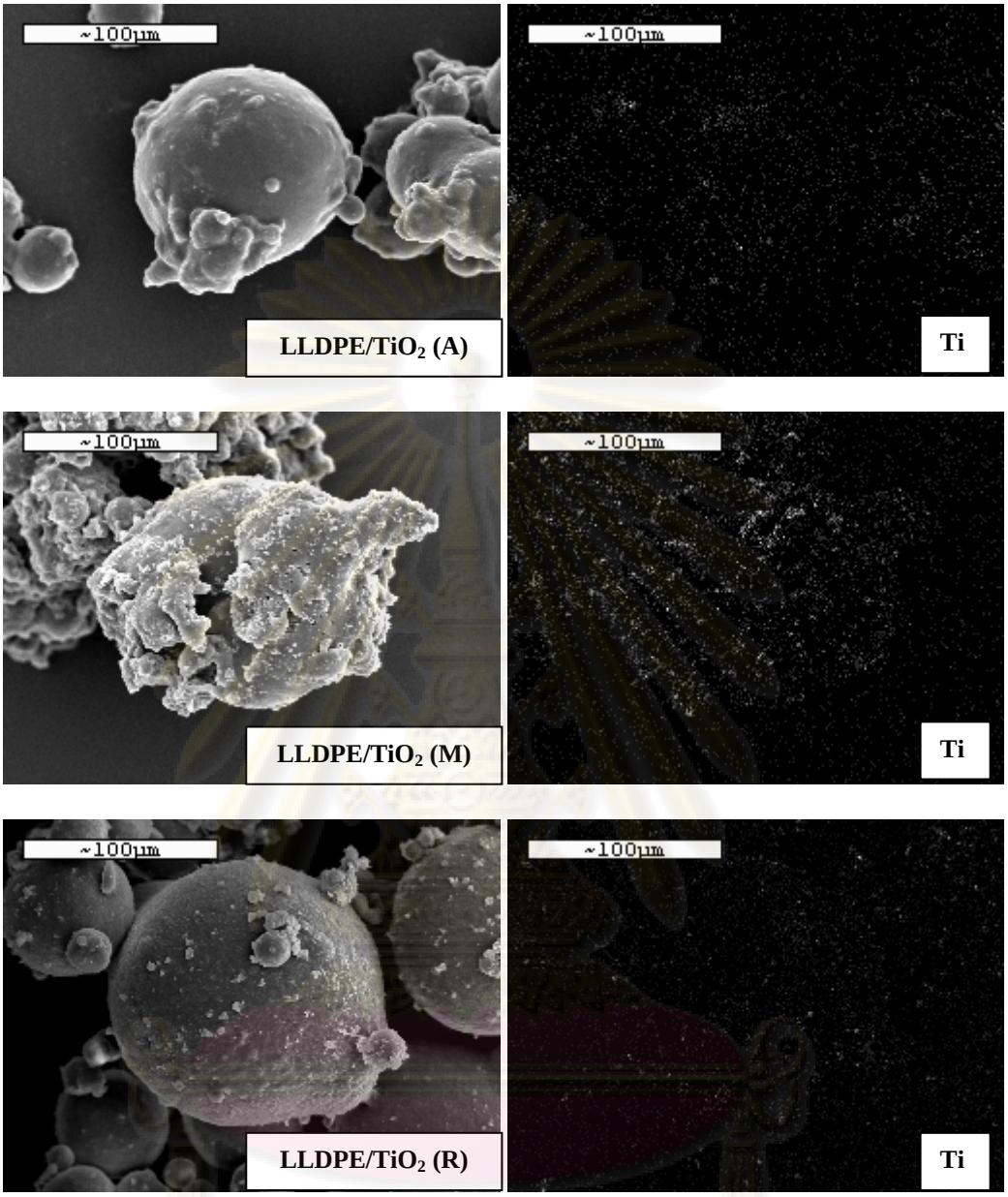

Figure 4.6 SEM micrographs of LLDPE/TiO_2 and Ti distribution obtained from EDX upon different TiO_2 supports

CHAPTER V

CONCLUSIONS & RECOMMENDATIONS

5.1 CONCLUSIONS

The copolymer of ethylene and 1-hexene were conducted using different TiO_2 supports via in situ polymerization with zirconocene/dMMAO catalyst. From the results of XPS, EDX and ICP of supports after impregnation, it revealed at the appearance of larger amount of $[Al]_{dMMAO}$ on the outer or external surface was observed. The TiO_2 support has a fragmentation after impregnated with dMMAO. The polymerization activities were in the order of TiO_2 (A) > TiO_2 (R) > TiO_2 (M) due to the more highly dispersion of the catalyst precursor and exhibits optimal interaction between $[Al]_{dMMAO}$ and TiO_2 (A). The low interaction is caused of the active sites were located on the outer surface more than pore resulting in leaching of active sites and low activity. The high insertion of comonomer is from the location of active sites was on the outer surface and the small particles for high surface area gave the highly dispersion of active sites. All copolymer obtained were random copolymer having different triad distribution and have a sphere shape.

5.2 RECOMMENDATIONS

- The modification of supports should be studied.
- Interaction between the support and cocatalyst under in situ condition should be further determined.
- Activity from the ratio of $[Al]_{dMMAO}/[Ti]_{support}$ from EDX and ICP should be further investigated.
- Re-run polymerization by using solvent from the first run to check the leaching of active site.
- Increase the ratio of ethylene/1-hexene to reduce the insertion of comonomer.

REFERENCES

[1] Li, K.T.; Dai, C.L. and Kuo, C.W. Ethylene polymerization over a nano-sized silica supported Cp_2ZrCl_2/MAO catalyst. **Catalysis Communications** 8 (2007): 1209-1213.

[2] Intaragamjon, N.; Shiono, T.; Jongsomjit, B. and Praserthdam, P. Elucidation of solvent effects on the catalytic behaviors for [t-BuNSiMe_2Flu]TiMe_2 complex during ethylene/1-hexene copolymerization. **Catalysis Communications** 7 (2006): 721-727.

[3] Desharun, C.; Jongsomjit, B. and Praserthdam, P. Study of LLDPE/alumina nanocomposites synthesized by in situ polymerization with zirconocene/d-MMAO catalyst. **Catalysis Communications** 9 (2008): 522-528.

[4] Britto, M.L.; Galland, G.B.; dos Santos, J.H.Z. and Forte, M.C. Copolymerization of ethylene and 1-hexene with $Et(Ind)_2ZrCl_2$ in hexane. **Polymer** 42 (2001): 6355-6361.

[5] Breslow, D. S. and Newburg, N. R. Bis-(cyclopentadienyl) titaniumdichloride-Alkylaluminum complexes as catalysts for the polymerization of ethylene. **Journal of American Chemical Society** 79 (1957): 5072-5073.

[6] Sinn, H. and Kaminsky, W. Ziegler-Natta Catalyst. **Advances in Organometallic Chemistry** 18 (1980): 99-149.

[7] Rodrigues, S.; Silveira, F.; dos Santos, J.H.Z. and Ferreira, M.L. An explanation for experimental behavior of hybrid metallocene silica-supported catalyst for ethylene polymerization. **Journal of Molecular Catalysis A: Chemical** 216 (2004): 19-27.

[8] Van Grieken, R.; Carrero, A.; Suarez, I. and Paredes, B. Ethylene polymerization over supported MAO/$(nBuCp)_2ZrCl_2$ catalysts: Influence of support properties. **European Polymer Journal** 43 (2007): 1267-1277.

[9] Kaminsky, W. The discovery of metallocene catalysts and their present state of the art. **Journal of Polymer Science Part A: Polymer Chemistry** 42 (2004): 3911-3921.

[10] Janiak, C. and Rieger, B. Silica gel supported zirconocene dichloride/methylaluminoxane catalysts for ethylene polymerization: Effects of heterogenation on activity, polymer microstructure and product morphology. **Angewandte Makromolekulare Chemie** 215 (1994): 47-57.

[11] Gallan, G.B.; Seferin, M.; Mauler, R.S. and Dos Santos, J.H.Z. Linear low-density polyethylene synthesis promoted by homogeneous and supported catalysts. **Polymer International** 48 (1999): 660-664.

[12] Bunchongturakarn, S.; Jongsomjit, B. and Praserthdam, P. Impact of bimodal pore MCM-41-supported zirconocene/dMMAO catalyst on copolymerization of ethylene/1-octene. **Catalysis Communications** 9 (2008): 789-795.

[13] Chaichana, E.; Jongsomjit, B. and Praserthdam, P. Effect of nano-SiO_2 particle size on the formation of LLDPE/SiO_2 nanocomposite synthesized via the *in situ* polymerization with metallocene catalyst. **Chemical Engineering Science** 62 (2007): 899-905.

[14] Ketloy, C.; Jongsomjit, B. and Praserthdam, P. Characteristics and catalytic properties of [t-BuNSiMe2Flu]$TiMe_2$/d-MMAO catalyst dispersed on various supports tpwards ethylene/1-octene copolymerization. **Applied Catalysis A: General** 327 (2007): 270-277.

[15] Unsitalo, A.M.; Pakkanen, T.T. and Iskola, E.I. Immobilization of metal chloride complexes of titanium, zirconium, and hafnium on a cyclopentadienyl surface of silica for ethylene polymerization. **Journal of Molecular Catalysis A: Chemical** 177 (2002): 179-194.

[16] Soga, K. and Kaminaka, M. Polymerization of propene with zirconocene-containing supported catalysts activated by common trialkylaluminums **Makromolekulare Chemie** 194 (1993): 1745-1755.

[17] Ko, Y.S.; Han, T.K.; Park, J.W. and Woo, S.I. Propene polymerization catalyzed over MCM-41 and VPI-5-supported $Et(ind)_2ZrCl_2$ catalysts. **Macromolecular Rapid Communications** 17 (1996): 749-758.

[18] Jongsomjit, B.; Kaewkrajang, P. and Praserthdam, P. Effect of silane-modified silica/MAO-supported $Et[Ind]_2ZrCl_2$ metallocene catalyst on copolymerization of ethylene. **European Polymer Journal** 40 (2004): 2813-2817.

[19] Margue, M.D.F.V. and Conte, A. The influence of the preparing conditions of SiO_2 supported Cp_2ZrCl_2 catalyst on ethylene polymerization. **Journal of Applied Polymer Science** 86 (2002): 2054-2061.

[20] Sensarma, S.; Sivaram, S. Polymerization of ethylene using a SiO_2-$MgCl_2$ supported bis(cyclopentadienyl)zirconium(IV) or titanium(IV) dichloride catalyst. **Polymer International** 51 (2002): 417-423.

[21] Belelli, P.G.; Ferreira, M.L. and Damiani, D.E. Silica-supported metallocene for ethylene polymerization. **Applied Catalysis A: General** 228 (2002): 189-202.

[22] Xu, J.T.; Zhu, Y.B.; Fan, Z.Q. and Feng, L.X. Copolymerization of propylene wwith various higher α-olefins using silica-supported *rac*-$Me_2Si(Ind)_2ZrCl_2$. **Journal of Polymer Science Part A: Polymer Chemistry** 39 (2001): 3294-3303.

[23] Koppl, A. and Alt, H.G. Heterogeneous metallocene catalysts for ethylene polymerization. **Journal of Molecular Catalysis A: Chemical** 165 (2001): 23-32.

[24] Korach, L. and Czaja, K. Synthesis and activity of metallocene catalysts supported on silica-type sol-gel carrier for ethylene polymerization. **Polymer Bulletin** 46 (2001): 67-74.

[25] Jongsomjit, B.; Praserthdam, P. and kaewkrajang, P. A comparative study on supporting effect during copolymerization of ethylene/1-olefins with silica-supported zirconocene/MAO catalyst. **Materials Chemistry and Physics** 86 (2004): 243-246.

[26] Wang, W.; Fan, Z.Q. and Feng, L.X. Ethylene polymerization and ethylene/1-hexene copolymerization using homogeneous and heterogeneous unbridged bisindenyl zirconocene catalysts. **European Polymer Journal** 41 (2005): 2380-2387.

[27] Tritto, I.; Boggioni, L.; Ravasio, A.; Zampa, C.; Hitkbleck, J.; Okuda, J.; Bredeau, S. and Dubios, P. Ethylene-norbornene copolymerization by rare-earth metal complexes and by carbon nanotube-supported metallocene catalysis. **Macromolecular Symposium** 260, (2007): 114-121.

[28] Paredes, B.; Soares, J.B.P.; Van Grieken, R.; Carrero, A. and Suarez, I. Characterization of ethylene-1-hexene copolymers made with supported metallocene catalysts: Influence of support type. **Macromolecular Symposium** 257 (2007): 103-111.

[29] Smedberg, A.; Hjertberg, T. and Gustafsson, B. Characterization of an unsaturated low-density polyethylene. **Journal of Polymer Science, Part A: Polymer Chemistry** 41 (2003): 2974-2984.

[30] Natta, G. and Plno, P. Crystalline high polymers of α-olefins. **Journal of the American Chemical Society** 77 (1955): 1708-1710.

[31] Gambarotta, S. Coord. Vanadium-based Ziegler-Natta: Challenges, promises, problems. **Coordination Chemistry Reviews** 237 (2003): 229-243.

[32] Ma, Y.; Reardon, D.F.; Gambarotta, S. and Yap, G.P.A. Vanadium-Catalyzed Ethylene-Propylene Copolymerization: The Question of the Metal Oxidation State in Ziegler-Natta Polymerization Promoted by (β-diketonate)$_3$V. **Organometallics** 18 (1999): 2773-2781.

[33] Kaminsky, W. and Laban, A. Metallocene catalysis. **Applied Catalysis A: General** 222 (2001): 47-61.

[34] Kashiwa, N. The discovery and progress of $MgCl_2$-supported $TiCl_4$ catalysts. **Journal of Polymer Science, Part A: Polymer Chemistry** 42 (2004): 1-8.

[35] Kissin, Y.V. Multicenter nature of titanium-based Ziegler-Natta catalysts: Comparison of ethylene and propylene polymerization reactions. **Journal of Polymer Science, Part A: Polymer Chemistry** 41 (2003): 1745-1758.

[36] Hlatky, G. Heterogeneous single-site catalysts for olefin polymerization. **Chemical Reviews** 100 (2000): 1347-1376.

[37] Natta, G.; Pino, P. and Mazzanti, G. A crystallizable organometallic complex containing titanium and aluminum. **Journal of the American Chemical Society** 79 (1957): 2975-2976.

[38] Arlman, E.J. and Cossee, P. Ziegler-Natta Catalysis III. Stereospecific Polymerization of Propene with th Catalyst System $TiCl_3$-$AlEt_3$. **Journal of Catalysis** 3 (1964): 99-104.

[39] Chung, T.-C.and Xu, G. US 6248837 B1, 2001 assigned to **The Penn State Research Foundation**

[40] Fujita, M.; Seki, Y. and Miyatake, T. Synthesis of Ultra-High-Molecular-Weight Poly(α-olefin)s by Thiobis(phenoxy)titanium/Modified Methylaluminoxane System. **Journal of Polymer Science, Part A: Polymer Chemistry** 42 (2004): 1107-1111.

[41] Kashiwa, N. and Imuta, J. Recent progress on olefin polymerization catalysts. **Catalysis Surveys from Japan** 1 (1997): 125-142.

[42] Sinclair, K. B. and Wilson, R. B. Metallocene catalysis - A revolution in olefin polymerization. **Chemistry & Industry** 7 (1994): 857-862.

[43] Gupta, V. K.; Satish, S. and Bhardwaj, I. S. Metallocene complexes of group 4 elements in the polymerization of monoolefins. **Journal of Macromolecular Science - Reviews in Macromolecular Chemistry and Physics** C34, No.3 (1994): 439-514.

[44] Naga, N. and Imanishi, Y. Copolymerization of ethylene and cyclopentene with zirconocene catalysts: Effect of ligand structure of zirconocenes. **Macromolecular Chemistry and Physics** 203 (2002): 159-165.

[45] Lauher, J. W. and Hoffmann, R. Structure and chemistry of bis(cyclopentadienyl)-MLn complexes. **Journal of the American Chemical Society** 98 (1976): 1729-1742.

[46] Castonguay, L. A.and Rappe, A. K. Ziegler-Natta catalysis. A theoretical study of the isotactic polymerization of propylene. **Journal of the American Chemical Society** 114 (1992): 5832-5842.

[47] Yang, X.; Stern, C. L. and Marks,T. J. "Cation-like" homogeneous olefin polymerization catalysts based upon zirconocene alkyls and tris(pentafluoropnenyl)borane. **Journal of the American Chemical Society** 113 (1991): 3623-3625.

[48] Chien, J. C. W. and Wang, B. P Metallocene-Methylaluminoxane catalysts for olefin polymerization. Trimethylaluminum as coactivator. **Journal of Polymer Science Part A: Polymer Chemistry** 26 (1988): 3089-3102.

[49] Pedeutour, J. N.; Radhakrishnan, K.; Cramail, H. and Deffieux, A. Use of "TMA-depleted" MAO for the activation of zirconocenes in olefin polymerization. **Journal of Molecular Catalysis A: Chemical** 185 (2002): 119-125.

[50] Pedeutour, J. N.; Cramail, H. and Deffieux, A. Influence of X ligand nature in the activation process of $racEt(Ind)_2ZrX_2$ by ethylaluminoxane. **Journal of Molecular Catalysis A: Chemical** 176 (2001): 87-94.

[51] Cam, D. and Giannini, U. **Makromolecular Chemistry** 193 (1992): 1049-1055.

[52] Soga, K.; Kim, H. J. and Shiono, T. Polymerization of ethylene with homogeneous metallocene catalysts activated by common trialkylaluminums and $Si(CH_3)_3OH$. **Macromolecular Rapid Communications** 14 (1993): 765-770.

[53] Katayama, H.; Shiraishi, H.; Hino, T.; Ogane, T., and Imai, A. The effect of aluminum compounds in the copolymerization alpha-olefins. **Macromolecular Symposia** 97 (1995): 109-118.

[54] Przybyla, C.; Tesche, B., and Fink, G. Ethylene hexene copolymerization with the heterogeneous catalyst system SiO_2/MAO/rac-Me_2Si[2-Me-4-h-Ind](2)$ZrCl_2$: The filter effect. **Macromolecular Rapid Communications** 20 (1999): 328-332.

[55] Harkki, O.; Lehmus, P.; Leino, R.; Luttikhedde, H. J. G.; Nasman, J. H. and Seppala, J. V. Copolymerization of ethylene with 1-hexene or 1-hexadecane over siloxy-substituted metallocene catalysts. **Macromolecular Chemistry and Physics** 200 (1999): 1561-1565.

[56] Cheruvu, S. **US Pat 5608019** (1997).

[57] Albano, C.; Sánchez, G., and Ismayel, A. Influence of a copolymer on the mechanical properties of a blend of PP and recycled and non-recycled DPE. **Polymer Bulletin** 41 (1998): 91-98.

[58] Shan, C.L.P.; Soares, J.B.P. and Penlidis, A. Ethylene/1-octene copolymerization studies with in situ supported metallocene catalysts: Effect of polymerization parameters on the catalyst activity and polymer microstructure. **Journal of Polymer Science Part A: Polymer Chemistry** 40 (2002): 4426-4451.

[59] Pietikainen, P. and Seppala, J.V. Low molecular weight ethylene/propylene copolymers. Effect of process parameters on copolymerization with homogeneous Cp_2ZrCl_2 catalyst. **Macromolecules** 27 (1994): 1325-1328.

[60] Soga, K. and Kaminaka, M. Polymerization of propene with the heterogeneous catalyst system $Et[IndH_4]_2ZrCl_2/MAO/SiO_2$ combined with trialkylaluminium. **Macromolecular Rapid Communications** 13 (1992): 221-224.

[61] Nowlin, T. E.; Kissin, Y. V. and Wagner, K. P. High activity Ziegler-Natta catalysts for the preparation of ethylene copolymers. **Journal of Polymer Science Part A: Polymer Chemistry** 26 (1988): 755-764.

[62] Chu, K. J.; Soares, J. B. P. and Penlidis, A**.** Variation of molecular weight distribution (MWD) and short chain branching distribution (SCBD) of ethylene/ 1-hexene copolymers produced with different in-situ supported metallocene catalysts. **Macromolecular Chemistry and Physics** 201 (2000): 340-348.

[63] Soga, K.; Uozumi, T.; Arai, T. and Nakamura, S. Heterogeneity of active species in metallocene catalysts. **Macromolecular Rapid Communications** 16 (1995): 379-385.

[64] De Fatima V.; Marques, M.; Conte, A.,; De Resende, F. C. and Chaves, E. G. Copolymerization of ethylene and 1-octene by homogeneous and different supported metallocenic catalysts. **Journal of Applied Polymer Science** 82 (2001): 724-730.

[65] Kim, J. D. and Soares, J. B. P. Copolymerization of ethylene and 1-hexene with supported metallocene catalysts: Effect of support treatment. **Macromolecular Rapid Communications** 20 (1999): 347-350.

[66] Chu, K. J.; Soares, J. B. P. and Penlidis, A. Polymerization mechanism for *in situ* supported metallocene catalysts. **Journal of Polymer Science Part : Polymer Chemistry** 38 (2000): 462-468.

[67] Chu, K.J.; Shan, C.L.P.; Soares, J.B.P. and Penlidis, A. Copolymerization of ethylene and 1-hexene with in-situ supported $Et[Ind]_2ZrCl_2$. Macromolecule **Chemical and Physics** 200 (1999): 2372-2376.

[68] Shan, C. L. P.; Chu, K. J.; Soares, J., and Penlidis, A. Using alkylaluminium activators to tailor short chain branching distributions of ethylene/ 1-hexene copolymers produced with in-situ supported metallocene catalysts. **Macromolecular Chemistry and Physics** 201 (2000): 2195-2202.

[69] Ribeiro, M. R.; Deffieux, A. and Portela, M. F. Supported metallocene complexs for ethylene and propylene polymerizations: preparation and activity. **Industrial and Engineering Chemistry Research** 36 (1997): 1224-1237.

[70] Chien, J. C. W. Supported metallocene polymerization catalysis. **Topic in Catalysis** 7 (1999): 23-36.

[71] Kaminsky, W. and Renner, F. High melting polypropylenes by silica supported zirconocene catalysts. **Macromolecular Chemistry Rapid Communication** 14 (1995): 239-243.

[72] Chien, J. C., and He, D. Olefin copolymerization with metallocene catalysts. II. Supported metallocene/methylaluminoxane catalyst for olefin Copolymerization. **Journal Polymer Science Part A: Polymer Chemistry** 29 (1991): 1603-1607.

[73] Chen, Y. X., Rausch, M. D., and Chien, J. C. Heptane soluble homogeneous zirconocene catalyst: Synthesis of a single diastereomer, polymerization catalysis, and effects of silica supports. **Journal Polymer Science Part A: Polymer Chemistry** 33 (1995): 2093-2108.

[74] Soga, K., and Kaminaka, M. Copolymerization of olefins with SiO_2-, Al_2O_3-, and $MgCl_2$-supported catalysts activated by trialkylaluminiums. **Macromolecular Chemistry and Physics** 195 (1994): 1369-1379.

[75] Soga, K., and Kaminaka, M. Polymerization of propene with a rac-$(CH_3)_2Si(2,4\text{-}(CH_3)_2C_5H_3)(3\ ,5\ \text{-}(CH_3)_2C_5H_3)ZrCl_2/MAO/SiO_2\text{-}Al\text{-}(iC_4H_9)_3$ catalyst system. **Macromolecular Rapid Communications** 15 (1994): 593-600.

[76] Soga, K., Arai, T., Nozawa, H., and Uozomi, T. Recent development in heterogeneous metallocene catalysts. **Macromolecular Symposia** 97 (1995): 53.

[77] Jin, J., Uozomi, T., Soga, K. Ethylene polymerization initiated by SiO_2-supported neodymocene catalysts. **Macromolecular Rapid Communications** 16 (1995): 317-322.

[78] Dominguez, A.M.; Zarate, A.; Quijada, R. and Lopez, T. Sol-gel iron complex catalysts supported on TiO_2 for ethylene polymerization. **Journal of Molecular Catalysis A: Chemical** 207 (2004): 155-161.

[79] Hagimoto, H.; Shiono, T. and Ikeda, T. Supporting Effects of Methylaluminoxane on the Living Polymerization of Propylene with a Chelating (Diamide)dimethyltitanium Complex. **Macromolecular Chemistry and Physics** 205 (2004): 19–26.

[80] Jiamwijitkul, S.; Jongsomjit, B. and Praserthdam, P. Effect of boron-modified MCM-41-supported dMMAO/zirconocene catalyst on copolymerization of ethylene/1-octene for LLDPE synthesis. **Iranian Polymer Journal** 16 (2007): 549-559.

[81] Jongsomjit, B.; Ngamposri, S and Praserthdam, P. Observation of bimodal polyethylene derived from TiO2-supported zirconocene/MAO catalyst during polymerization of ethylene and ethylene/1-hexene. **Catalysis Letters** 117 (2007): 177-181.

[82] Jongsomjit, B.; Kaewkrajang, P.; Wanke, S.E. and Praserthdam, P. A comparative study of ethylene/α-olefin copolymerization with silane-modified silica-supported MAO using zirconocene catalysts. **Catalysis Letters** 94 (2004): 205-208.

[83] Jongsomjit, B.; Ngamposri, S. and Praserthdam, P. Catalytic activity during copolymerization of ethylene and 1-hexene via mixed TiO_2/SiO_2-supported MAO with rac-$Et[Ind]_2ZrCl_2$ metallocene catalyst. **Molecules** 10 (2005): 672-678.

[84] Severn, J.R.; Chadwick, J.C.; Duchateau, R. and Friderichs, N. “Bound but Not Gagged"-Immobilizing Single-Site α-Olefin Polymerization Catalysts. **Chemical Review** 105 (2005): 4073-4147.

[85] Randall, J. C. A review of high resolution liquid ^{13}C nuclear magnetic resonance characterization of ethylene-based polymers. **Journal of Macromolecular Science, Reviews in Macromolecular Chemistry and Physics** C29 (1989): 201-315.

[86] Galland G.B.; Quijada P.; Mauler R.S. and De Menezes S.C. Determination of reactivity ratios for ethylene/α-olefin copolymerization catalysed by the $C_2H_4[Ind]_2ZrCl_2$/methylaluminoxane system. **Macromolecular Rapid Communications** 17 (1996): 607-613.

APPENDICES

APPENDIX A

(X-ray photoelectron spectroscopy)

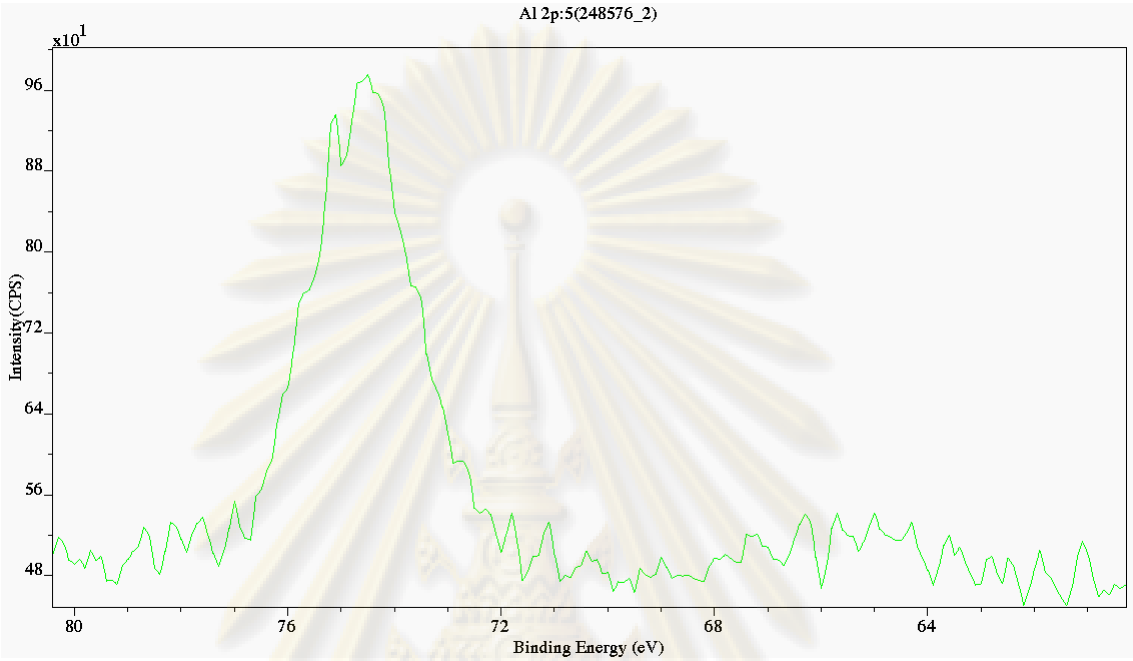

Figure A-1 XPS spectra of Al_{2p} on TiO_2 (A)

Table A-1 Binding energy (BE) and % mass concentration of catalyst precursor [TiO_2 (A)]

Peak	Position BE (ev)	FWHM (ev)	Atomic Mass	Atomic Conc %	Mass Conc %
O_{1s}	532.0	3.048	15.999	48.31	47.51
Ti_{2p}	459.0	1.456	47.878	0.12	0.35
C_{1s}	285.0	2.584	12.001	36.29	26.79
Al_{2p}	74.5	1.970	26.982	15.28	25.35

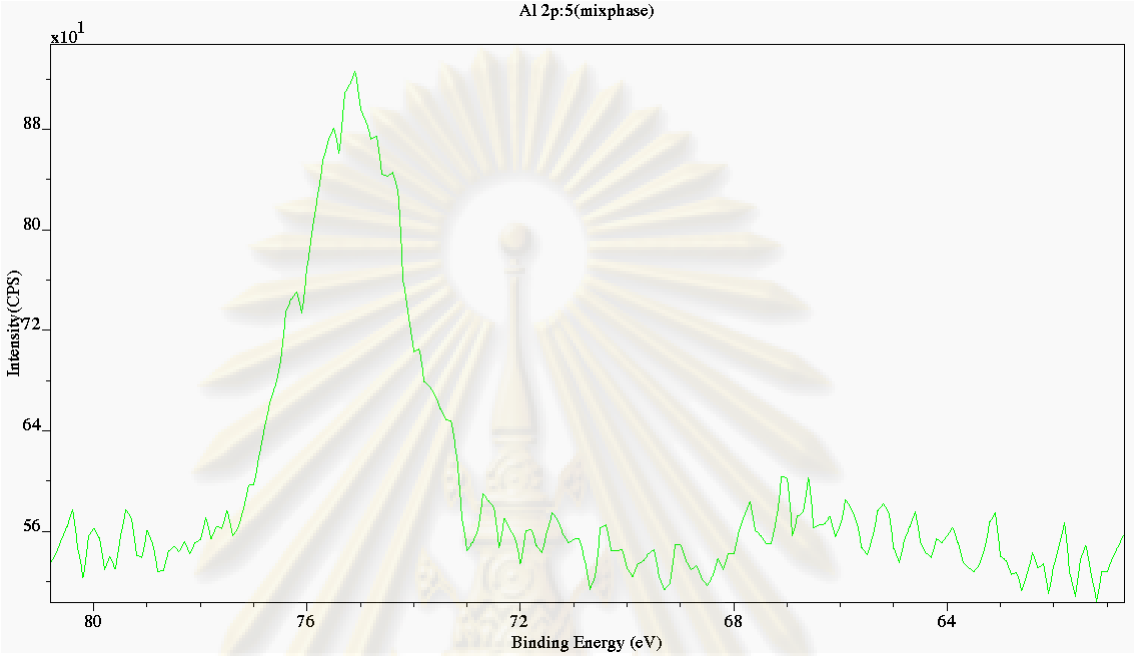

Figure A-2 XPS spectra of Al_{2p} on TiO_2 (M)

Table A-2 Binding energy (BE) and % mass concentration of catalyst precursor [TiO_2 (M)]

Peak	Position BE (ev)	FWHM (ev)	Atomic Mass	Atomic Conc %	Mass Conc %
O_{1s}	532.6	2.854	15.999	38.29	41.14
Ti_{2p}	459.4	1.143	47.878	0.08	0.26
C_{1s}	285.0	2.233	12.011	52.77	42.56
Al_{2p}	75.1	2.143	26.982	8.86	16.05

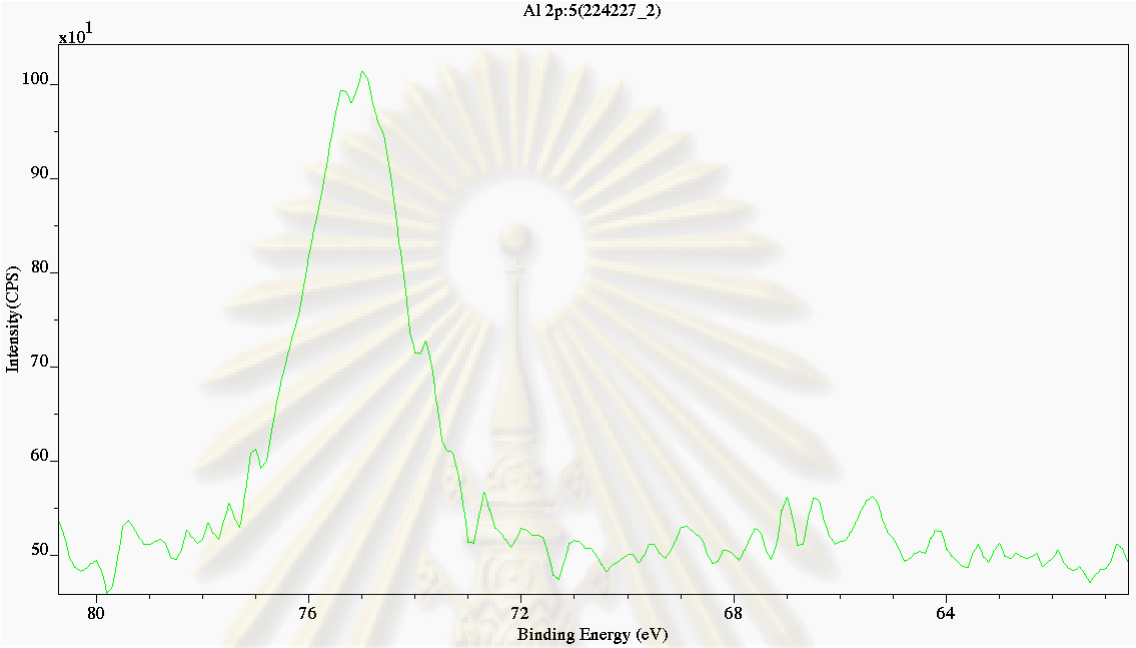

Figure A-3 XPS spectra of Al_{2p} on TiO_2 (R)

Table A-3 Binding energy (BE) and % mass concentration of catalyst precursor [TiO_2 (R)]

Peak	Position BE (ev)	FWHM (ev)	Atomic Mass	Atomic Conc %	Mass Conc %
O_{1s}	532.4	2.993	15.999	44.41	45.29
Ti_{2p}	459.2	0.879	47.878	0.05	0.16
C_{1s}	285.0	2.425	12.001	42.92	32.86
Al_{2p}	75.0	1.905	26.982	12.62	21.70

APPENDIX B

(Energy dispersive x-ray spectroscopy)

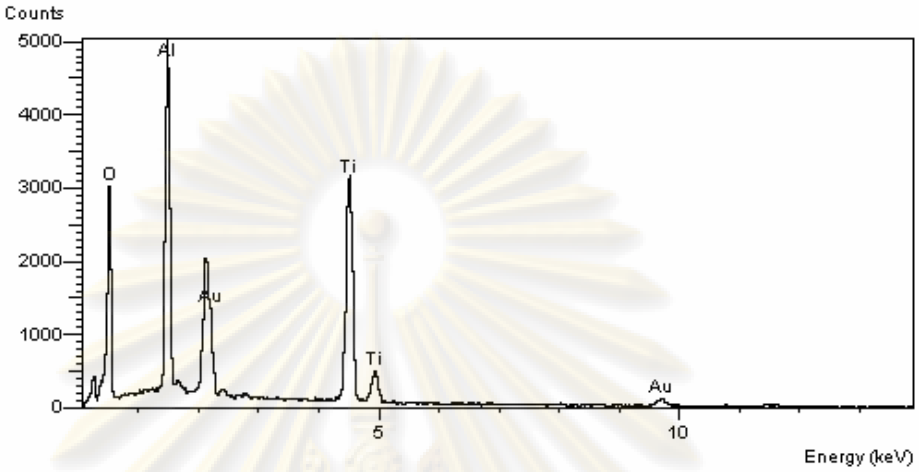

Figure B-1 EDX profiles of $[Al]_{dMMAO}$ on TiO_2 (A) supports

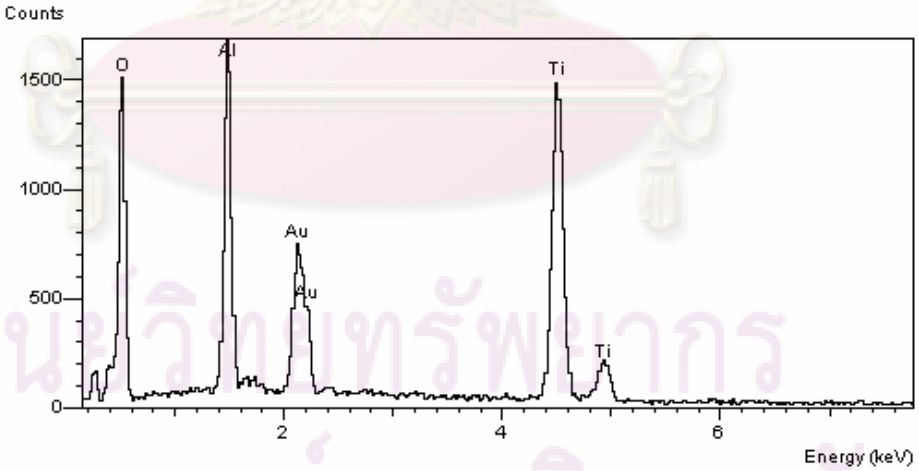

Figure B-2 EDX profiles of $[Al]_{dMMAO}$ on TiO_2 (M) supports

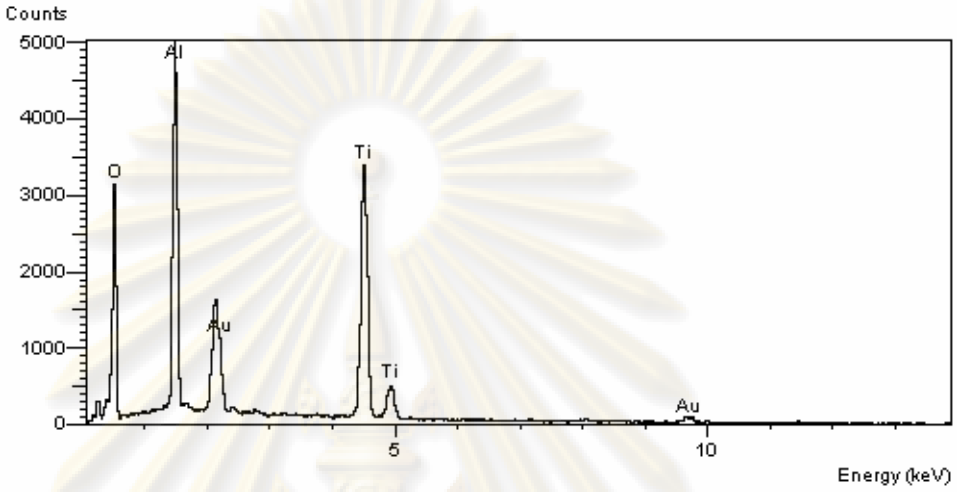

Figure B-3 EDX profiles of $[Al]_{dMMAO}$ on TiO_2 (R) supports

APPENDIX C

(Differential Scanning Calorimeter)

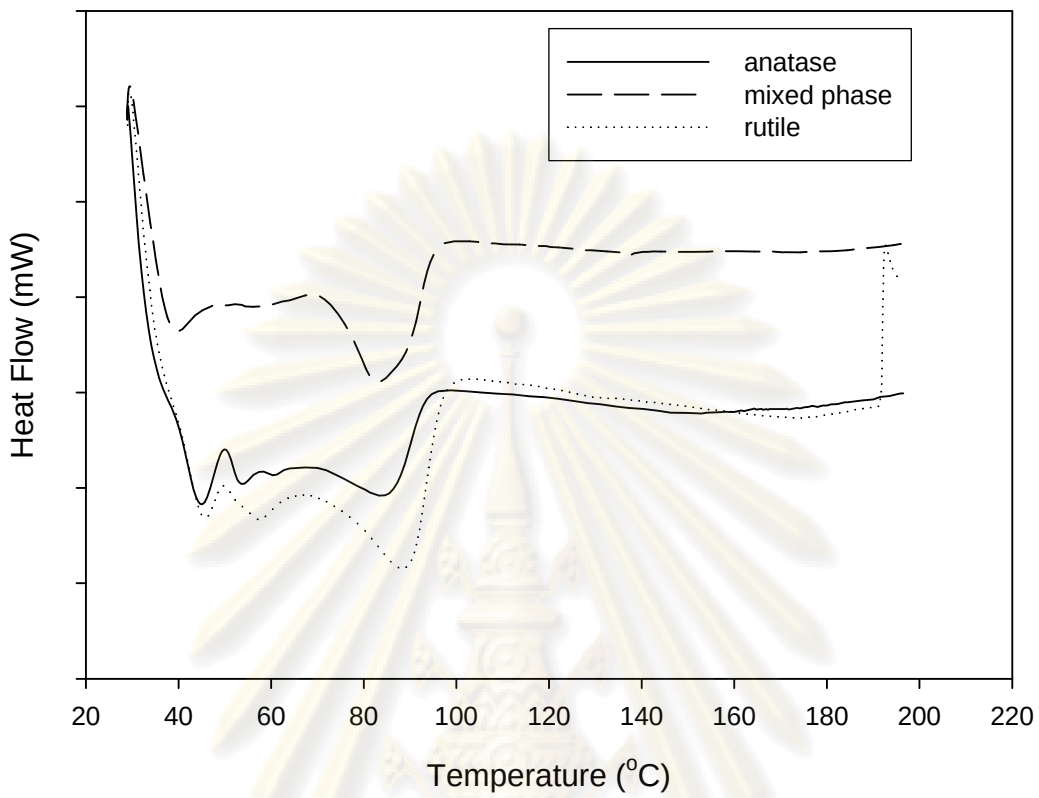

Figure C-1 DSC curve of LLDPE/TiO_2 copolymer at Al/Zr = 1135

APPENDIX D
(Calculation of polymer properties)

D-1 Calculation of polymer microstructure

Polymer microstructure and also triad distribution of monomer can be calculated according to the Galland G.B. [90]. in the list of reference. The detail of calculation for ethylene/α-olefin copolymer was interpreted as follow.

1-Hexene

The integral area of ^{13}C-NMR spectrum in the specify range are listed.

T_A	=	39.5 - 42	ppm
T_B	=	38.1	ppm
T_C	=	33 - 36	ppm
T_D	=	28.5 - 31	ppm
T_E	=	26.5 – 27.5	ppm
T_F	=	24 - 25	ppm
T_G	=	23.4	ppm
T_H	=	14.1	ppm

Triad distribution was calculated as the followed formula.

k[HHH]	=	$2T_A - T_C + T_G + 2T_F + T_E$
k[EHH]	=	$2T_C - 2T_G - 4T_F - 2T_E - 2T_A$
k[EHE]	=	T_B
k[EEE]	=	$0.5T_D - 0.5T_G - 0.25T_E$
k[HEH]	=	T_F
k[HEE]	=	T_E

APPENDIX E

(Nuclear Magnetic Resonance)

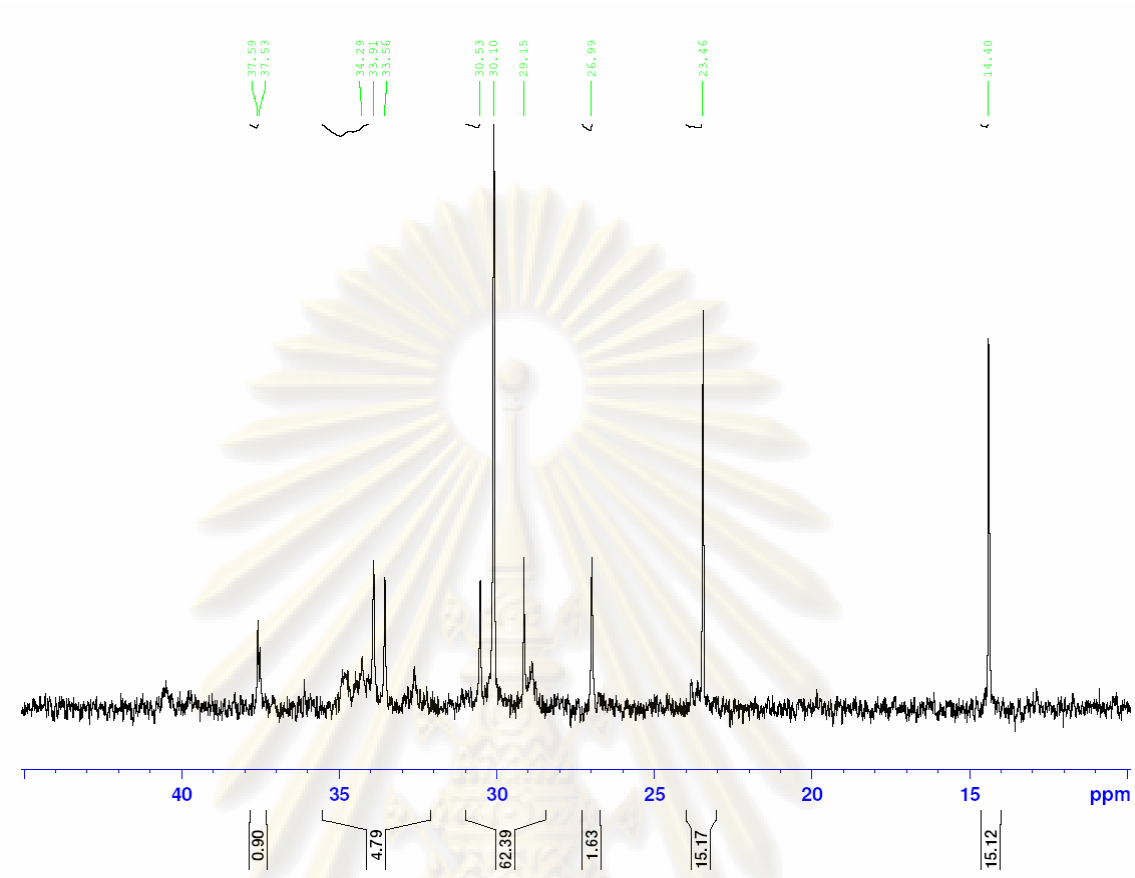

Figure E-1 ^{13}C NMR spectrum of ethylene/1-hexene copolymer produce with homogenous

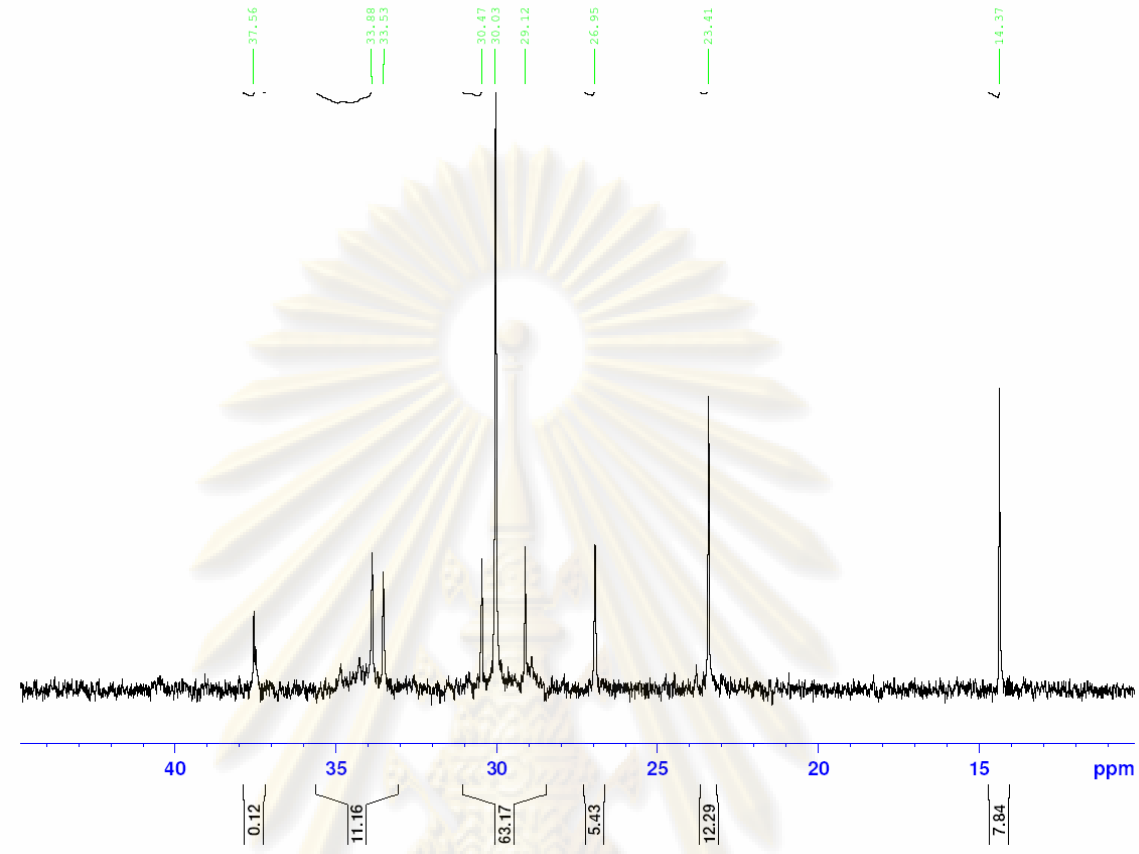

Figure E-2 ^{13}C NMR spectrum of ethylene/1-hexene copolymer produce with TiO_2 (A)

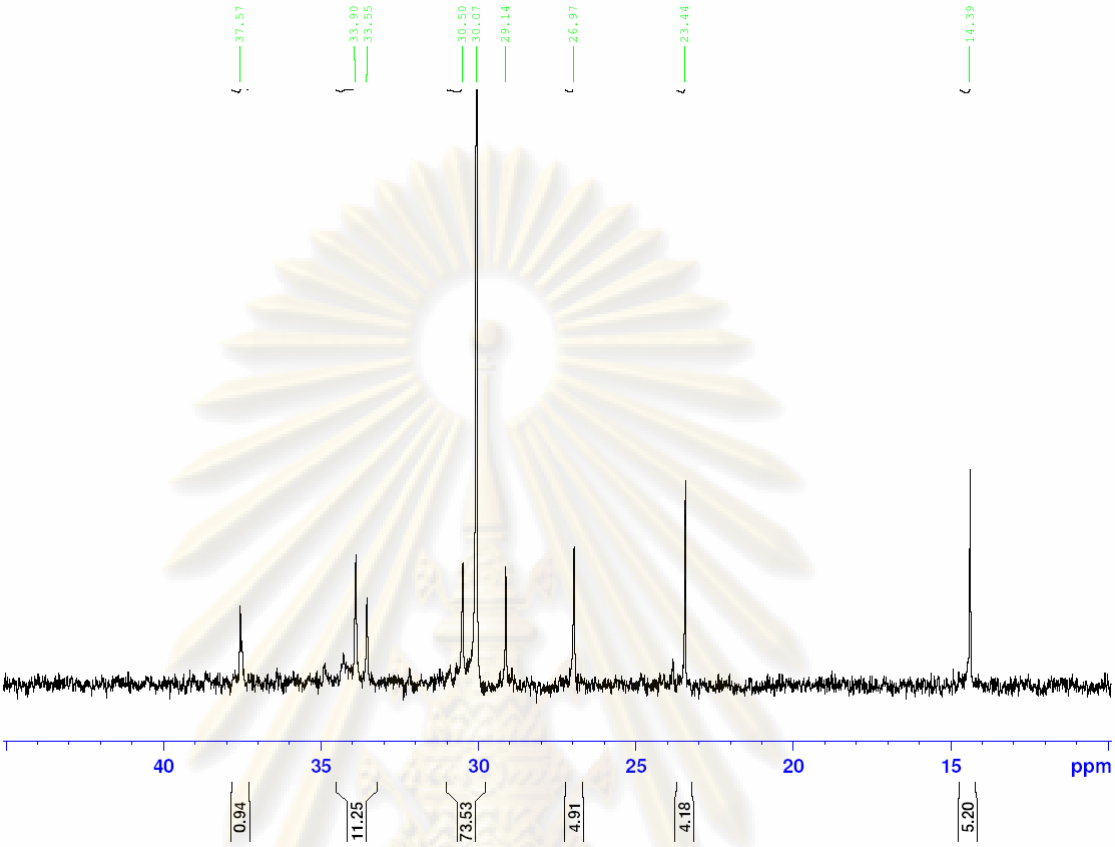

Figure E-3 ^{13}C NMR spectrum of ethylene/1-hexene copolymer produce with TiO_2 (M)

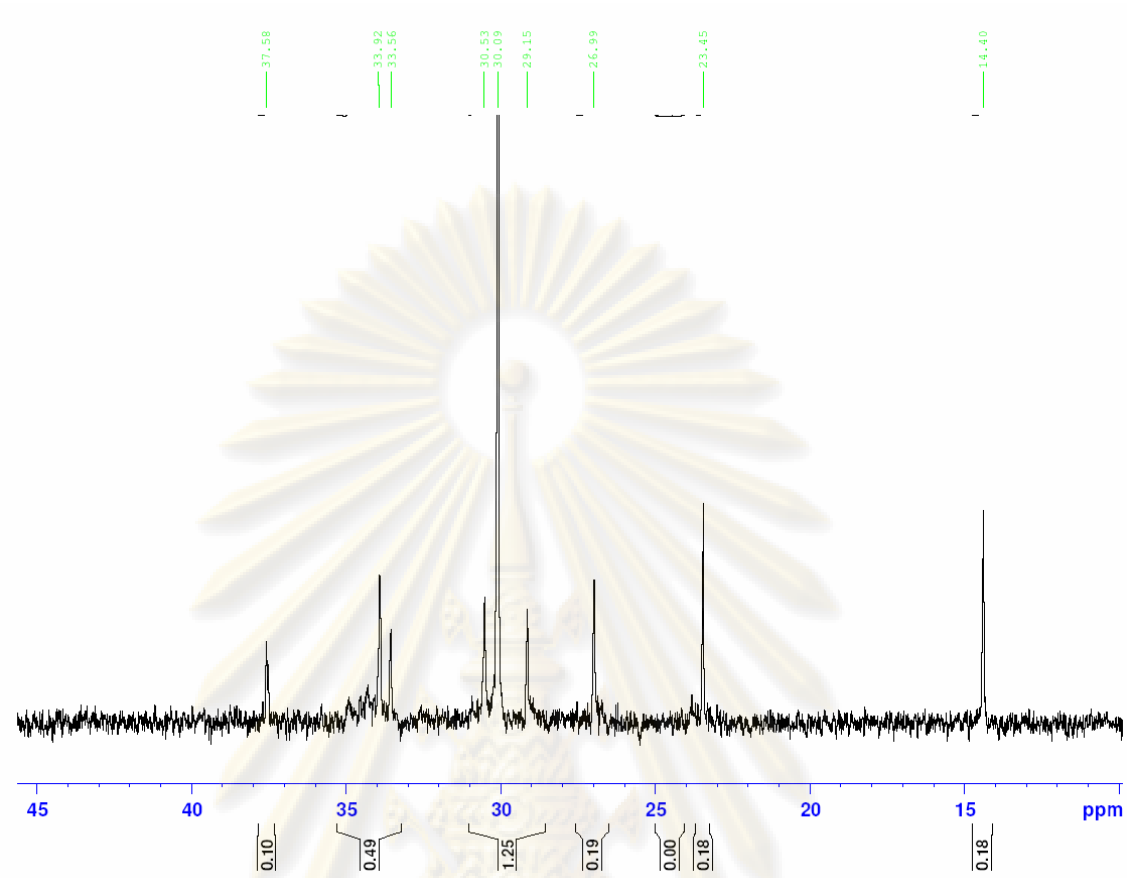

Figure E-4 ^{13}C NMR spectrum of ethylene/1-hexene copolymer produce with TiO_2 (R)

APPENDIX F

(LIST OF PUBLICATION)

1. Sriphaisal, T. and Jongsomjit, B. “Effect of titania-supported metallocene catalyst for LLDPE production” (The Proceeding of 18th Thailand Chemical Engineering and Applied Chemistry Conference, TIChe 2008, Pattaya)

VITA

Mr.Thanai Sriphaisal was born on August 3, 1982 in Bangkok, Thailand. He received the Bachelor's Degree of Chemical Engineering from the Department of Chemical Engineering, Faculty of Engineering, King Mongkut Institute of Technology Lardkrabang in March 2003, he continued his Master's study at Chulalongkorn University in June, 2007.